Identification of Recharge Source Areas in a Fractured Crystalline-rock Aquifer in Ploemeur, France

Cathleen Hana Humm

Thesis submitted to the faculty of the Virginia Polytechnic Institute and State University in partial fulfillment of the requirements for the degree of

Master of Science
In
Geosciences

Thomas J. Burbey
Ryan Pollyea
Mark Widdowson

May 6, 2021
Blacksburg, VA

Keywords: (groundwater, recharge, fractured crystalline-rock aquifer, numerical model)

Identification of Recharge Source Areas in a Fractured Crystalline-rock Aquifer in Ploemeur, France

Cathleen Hana Humm

ABSTRACT

Characterizing and preserving available groundwater resources within crystalline rocks is pertinent to understanding and predicting resources for ecosystems worldwide. Crystalline-rock aquifers, with favorable structure and climate, can be pumped year round to meet local domestic demand. The Ploemeur hydrogeologic site, near the southern coast of Brittany, France, is characterized by a structurally complex fractured mica-schist and granite confined aquifer system. A contact zone, which acts as the main localized flow path through the aquifer, separates the two crystalline units, and a sub-vertical permeable fault zone cross cuts the crystalline bedrock and contact zone. Using field observations, recharge estimates, and a calibrated three-dimensional numerical multi-zone MODFLOW 6 model, we present preferential flow paths of recharge infiltrating the complex geology of the Ploemeur hydrogeological site during pumping conditions. Using MODPATH to track groundwater and recharge path lines, we determine that water extracted from the aquifer originates from higher elevation areas west of the pumping site. Particle tracking analyses indicate that precipitation simulated over the pumping zone takes a minimum of two years to reach the pumping wells and travels up to 100 m in distance. Analyses of the water budget of the aquifer system using Zonebudget show that storage contributes significantly to the productivity of the system. Based on these analyses, we determine that recharge mechanisms such as piston flow and preferential flow play important roles in the Ploemeur hydrogeologic site. Though the Ploemeur site is unique in its composition and geometry, the methods used to characterize and monitor the aquifer can be applied to fractured crystalline-rock aquifers globally. Fractured

crystalline-rock aquifers make up 10% of the region's freshwater sources, thus understanding their flow mechanisms contributes greatly to the management of freshwater resources.

Identification of Recharge Source Areas in a Fractured Crystalline-rock Aquifer in Ploemeur, France

Cathleen Hana Humm

GENERAL AUDIENCE ABSTRACT

Groundwater aquifers are a common source of freshwater worldwide as groundwater makes up 30% of Earth's freshwater resources. Porous, sedimentary aquifers, made of materials such as sand or gravel, are well studied; however, the less understood aquifers found in crystalline bedrock are also found all over the world. Generally, igneous and metamorphic crystalline rocks are not porous and have low permeabilities, but fractures and faults in the crystalline rock can increase the ability for water to travel through the system. The Ploemeur hydrogeologic site, located on the southern coast of Brittany, France, is a productive fractured crystalline-rock groundwater aquifer producing freshwater year round. The productivity of this aquifer is attributed to the increased hydraulic conductivity associated with the intersection of two permeable features: a subvertical fault zone and a sub-horizontal contact zone. Despite the aquifer's output, recharge travels very slowly into the system due to the depth, heterogeneity, and clay content in an overlying layer of weathered rock fragments and soil. In this study, we create a three-dimensional numerical model using MODFLOW to simulate precipitation in different locations to see how it travels through the aquifer to the site of groundwater pumping. We see that the recharge prefers to travel topographically from regions of higher elevation to lower elevation. The recharge preferentially travels through the geologic features with higher permeabilities, including the fault zone, regolith, and contact zone, but it does still travel through the less permeable, crystalline bedrock units. Even in the features with the higher permeabilities, simulated recharge requires a minimum of 2 years to travel from the land surface to the pumping wells. The pumping wells extract significant water from storage, as seen in our water budget calculations of each geologic unit. We see two recharge

mechanisms present in the hydrogeologic site: piston flow, where young water displaces older water from the storage, and preferential flow, where recharge prefers to travel through regions with higher hydraulic conductivity. Understanding the recharge mechanisms in crystalline aquifers is pertinent to our knowledge of freshwater resources as crystalline aquifers make up approximately 10% of all groundwater supplies.

ACKNOWLEDGEMENTS

First and foremost, I would like to express my gratitude to my advisor, Dr. Tom Burbey, for his continuous support and advice on this research project and beyond. I truly appreciate the opportunity he provided me to continue my education at Virginia Tech and expand my knowledge of hydrogeologic processes and numerical modeling. I have learned a lot during my two years working and taking classes with Dr. Burbey, and I am looking forward to applying this knowledge as I begin my career.

Thank you to Dr. Ryan Pollyea and Dr. Mark Widdowson for agreeing to serve as committee members to provide feedback on my research project and academic progress. Your feedback and questions have been helped make my research project what it is today.

Thank you to the Department of Geosciences at Virginia Tech for the funding in the form of the Leo and Melva Harris Summer Scholarship as well as the funding and support to serve as a teaching assistant. The community in the department is motivating and inspiring, and I will cherish the memories and friendships I have made during my time at Virginia Tech.

Lastly, thank you to my parents and my support system of friends and peers for their constant encouragement and support surrounding my research and academic endeavors.

TABLE OF CONTENTS

LIST OF FIGURES

LIST OF TABLES

INTRODUCTION

Groundwater is an often necessary resource to support populations, both urban and rural, industry, and agriculture with freshwater (Ali and Mubarak, 2017). Though groundwater is a renewable resource, it can take many months to years for an aquifer to replenish enough groundwater to be a dependable resource (Ali and Mubarak, 2017). The ability to characterize and predict recharge rates in our freshwater resources is more critical now than ever as increasing temperatures from recent changes in climate affect surface tension and other matric properties reducing the ability for groundwater aquifers to hold water (Nimmo, 2005, Scibek et al., 2007; Green et al., 2011; Aquilina et al., 2015). Therefore, proper monitoring and management of the reservoirs, particularly those providing groundwater to towns and cities, is critical to supplying enough freshwater to those dependent on the resources. However, the fractured crystalline-rock makeup of some groundwater aquifers, including the Ploemeur hydrologic site in this study, provide additional challenges and uncertainties in the management and prediction of these aquifers.

It is estimated that one-third of Earth's crust is composed of igneous and metamorphic bedrock (Blatt and Jones, 1975; Amiotte-Suchet et al., 2003; Gleeson et al., 2012). Fractured rock aquifers are found around the world (Maréchal et al., 2004; Gleeson et al., 2009; Pedretti et al., 2016; Dewandel et al., 2012; Maréchal et al., 2018), but they are less understood than porous aquifers. This is due to their heterogenous nature locally, regionally, and worldwide which makes them difficult to quantify and compare to other similar aquifers (Cook, 2003; Roques et al., 2016). Contrary to the permeable nature of aquifers composed of unconsolidated sediments, crystalline rocks, notably mica-schist and granite, are not typically considered good aquifers or reservoirs due to their close crystalline structures and extremely low primary permeabilities. However, faulting

and fracturing from weathering and tectonic activity can increase the secondary permeability and thus the ability to transmit water (Aquilina et al., 2004; Bense et al., 2013). Deformation in shallow (< 1 km) crust increases the permeability, heterogeneity, and anisotropy of the geology, sometimes creating a layer of regolith at the ground surface (Bense et al., 2013). Water can travel through fractures more quickly than the crystalline matrix, and water preferentially travels through a path of least resistance (Nimmo, 2005). The impacts of fractures and faults on groundwater systems varies by location due to heterogeneity in climate, geology, and topography among other factors (Bense et al., 2013). If a fractured rock aquifer contains substantial interconnected fractures to transport enough water to support local need, it can be considered an aquifer.

Other factors including climate, topography, and soil properties can play significant roles in the productivity of fractured crystalline rock aquifers. Recharge, or water supplying a groundwater reservoir or aquifer, is considered one of the most important factors in determining the productivity of an aquifer (Lerner et al, 1990; Scanlon et al., 2002; Gleeson et al., 2009; Leray et al., 2013; Ali and Mubarak, 2017). However, accurately quantifying recharge is difficult due to factors such as natural heterogeneity in the hydraulic parameters of the soil and geologic materials as well as the complexities from the overlying and surrounding vegetation (Lerner et al., 1990; Scanlon et al., 2002; Nimmo, 2005; Gleeson et al., 2009; Ali and Mubarak, 2017). Surface recharge, such a runoff and precipitation, often travels to streams and other surface water bodies following topography from higher elevations to lower elevations. After penetrating the ground surface, recharge is assumed to travel vertically downward to reach the aquifer (Ali and Mubarak, 2017), though this vertical flow may be impeded depending on the hydraulic parameters of the soil and regolith and layers overlying the aquifer.

Groundwater models provide insight to the conceptual behavior of flow and transport through an aquifer system (Cook, 2003; Ali and Mubrarak, 2017). Numerical modeling of groundwater systems represents a tool that allows for analyses and studies that could not be made in the field due to an aquifer's depth, heterogeneity, or connectivity among other factors (Le Borgne et al., 2004; Nimmo, 2005). Environmental models are important to manage and predict natural resources, such as freshwater, particularly to see how a groundwater system responds to environmental and anthropogenic changes (White et al., 2020). Many models, particularly those representing a specific site, contain observations and hydraulic parameter estimations from field analyses, as large numbers of hydrogeologic observations and accurate parameter estimations are important for model calibration (Cook, 2003; Leray et al., 2012; Ali and Mubarak, 2017). However, numerical modeling typically results in conclusions that are non-unique, or results that could be true for a variety of geological sites and models even if the sites differ in geology and geometry (Berkowitz, 2002; Cook, 2003; Le Borgne et al., 2004). To ensure a model accurately represents the geologic system of interest for the intended modeling purpose, it should reflect the controlling features, boundary conditions, and the scale of interest for the region (Cook, 2003). The heterogenetic nature and localized flow patterns of water through fractured crystalline-rock aquifers challenges conventional numerical groundwater models; however, adaptations to current methods are made to both decrease the complexities of the groundwater systems and increase the complexities of the models to fit the groundwater system being modeled (Maréchal et al., 2018).

The hydrogeologic site investigated in this study is a fractured crystalline-rock aquifer located in Ploemeur, France. Geology at the site consists of faulted and fractured granite and mica-schist separated by a sub-horizontal contact zone. Despite its uncharacteristic makeup for a prolific aquifer, the Ploemeur hydrogeologic site is able to supply consistent freshwater to over 20,000

inhabitants with limited groundwater drawdown. Due to the fractured and heterogenous crystalline-rock that makes up the Ploemeur hydrogeologic site, it is difficult to understand the nature of recharge and groundwater flow in the hydrogeologic system, particularly at depth and in the unfractured matrix. In this study, we investigate the hydrogeologic mechanisms that contribute to the productivity of the site with a three-dimensional numerical model created with MODFLOW 6 and ModelMuse. Specifically, we seek to determine the sources of the groundwater extracted through the pumping wells during average recharge and pumping conditions. The numerical model simulates which geologic units the recharge prefers to flow through while traveling to the pumping wells. This study contributes to the understanding of hydromechanical and temporal properties driving groundwater flow and recharge in the Ploemeur aquifer. Additionally, the findings in this study provides new understanding of these flow mechanisms that allow for improved groundwater management in fractured and faulted crystalline-rock aquifers worldwide.

BACKGROUND

Recharge

Recharge is a pertinent factor in determining whether a groundwater aquifer will be a productive water resource to supply local needs; therefore, estimating current recharge and predicting future recharge rates is essential for maintaining sustainable water resources management (Lerner et al., 1990; Scanlon et al., 2002; Cook, 2003; Gleeson et al., 2009; Baker and Miller, 2013; Ali and Mubarak, 2017). Recharge is often the limiting factor in quantifying sustainable groundwater extraction rates (Leray et al., 2013). Aspects of proper recharge estimation include understanding an aquifer's water budget through sources of recharge and discharge, preferential flow paths, climate, and impacts of local geology (Cook, 2003; Ali and Mubarak, 2017). Natural recharge and discharge cycles are controlled by the regional climate and can vary by year, season, or decade (Biessy et al., 2011). The regional geology can also play a significant role as the quantity of recharge per unit area that can be stored for later use during the seasons or during periods of increased pumping is dependent on the hydrologic properties of the geologic units (Ruelleu et al., 2010; Leray et al., 2012, 2013; Bense et al., 2013; Jiménez-Martínez et al., 2013; Roques et al., 2014, 2016; Ali and Mubarak, 2017). Despite the importance of recharge in characterizing groundwater resources in groundwater aquifers, recharge rates are often difficult to accurately quantify.

Recharge can originate from a variety of sources, including precipitation, runoff, storage of adjacent geologic units and reservoirs, ponding in lower topographic areas, artificial recharge, or leakage from nearby surface water features (Lloyd, 1986; Sukhija et al., 2003). Meteoric water, or water originating from precipitation, is a common source of natural recharge for groundwater aquifer systems as it can travel through the unsaturated zone to the water table, replenish surface

water bodies, or freeze as ice. Surface water bodies, such as streams, lakes, and ponds, lose water to groundwater aquifers when the water table level falls below the surface water level at any location beneath the surface water feature, otherwise known as induced recharge (Winter et al., 1998; Ali and Mubarak, 2017). Irrigation water from agricultural regions can re-enter the subsurface during dry seasons (Mustafa et al., 2017). In colder regions, snowmelt at the end of the winter months recharges the groundwater system, most notably in aquifers with shallow water tables (Buttle and Sami, 1990; Gleeson et al., 2009). Recharge occurs intensely and rapidly during periods of glacial melt, which can be determined from analyzing deep groundwater extracted from aquifers in across Europe (Klump et al., 2008; Gleeson et al., 2009 Alvarado et al., 2011; Aquilina et al., 2015). Urban recharge includes leaks from infrastructure for water supply and sewage networks (Lerner, 2002; Wakode et al., 2018). Artificial recharge occurs when water is pumped into a reservoir in an effort to prevent the deleterious effects of over-pumping such as land subsidence and related earth fissures (Ali and Mubarak, 2017).

As recharge infiltrates into a groundwater system, it is typically assumed to travel vertically through the unsaturated zone (Ali and Mubarak, 2017). When it reaches groundwater in the saturated zone, it can travel vertically or horizontally depending on the local hydraulic gradient and geologic conditions (Winter et al., 1998). Diffuse recharge is common in humid-zone climates. Diffuse recharge refers to a process whereby precipitation occurs over a large spatial area and travels vertically through the unsaturated zone to the water table by gravity drainage (Healy, 2010; Ali and Mubarak, 2017). Piston flow describes the instances when new recharge displaces older water stored in the unsaturated or saturated zones, forming regions of different-aged water (Hewlett and Hibbert, 1967; Zimmermann et al., 1967; Buttle and Sami, 1990; Sukhija et al., 2003; Ali and Mubarak, 2017). Piston flow has been documented in both homogeneous medium porous

media and fractured crystalline-rock (Zimmermann et al., 1967; Sukhija et al., 2003), but this flow process is not always the primary recharge mechanism in fractured hard rock aquifers (Sukhija et al., 2003). Instead, recharge in heavily faulted or jointed rocks often follows a path of least resistance, or preferential flow paths, through interconnected fracture orientations with higher permeability and connectivity than surrounding low permeability rock (Sukhija et al., 2003; Nimmo, 2005; Gleeson et al., 2009; Pedretti et al., 2016; Roques et al., 2016; Ali and Mubarak. 2017; Schuite et al., 2017). Preferential flow paths are influenced by such factors as the connectivity and size (aperture) of the fractures and overall volumetric water content (Cook, 2003; Nimmo, 2005; Gleeson et al., 2009). Inter-aquifer flow, or groundwater underflow, occurs when leakage from an overlying aquifer travels through a semi-permeable layer into a separate aquifer (Healy, 2010). Although this occurrence is not always considered recharge, it is important to consider when calculating the water balance of an aquifer system (Lerner, 1990).

Accurately estimating recharge through a groundwater aquifer is imperative for the understanding and sustainable management of the reservoir (Lerner et al., 1990; Scanlon et al., 2002; Gleeson et al., 2009; Ali and Mubarak, 2017). However, measuring or accurately quantifying recharge remains one of the biggest challenges in hydrogeology as the most precise methods for acquiring subsurface data from percolating water are expensive and complex (Lerner et al., 1990; Scanlon et al., 2002; Nimmo; 2005; Ali and Mubarak, 2017). Such complexity is due to natural heterogeneity in the hydraulic parameters of the soil and geologic materials as well as the complexities that influence the available recharge from the overlying and surrounding vegetation (Nimmo, 2005; Gleeson et al., 2009; Ali and Mubarak, 2017). Additionally, determining recharge over a specific spatial location is challenging due to temporal changes and complications with seasonal, decadal, or long-term weather and climate changes (Healy, 2010).

The water table can also fluctuate from air entrapment, bank-storage effects near surface streams and rivers, tidal effects near oceans, pumping conditions, and deep-well injections, all without considering changes in recharge (Freeze and Cherry, 1979).

In order to account for the complexity of factors influencing groundwater recharge, efforts have been made to outline simpler methodologies for estimating recharge. Common and easily measured parameters, such as soil moisture content, hydraulic conductivity, water table and potential head fluctuations, evapotranspiration, and recharge extinction depth, are used to estimate recharge and infiltration in groundwater systems (Lerner et al., 1990; Lee et al., 2006; Healy, 2010; Ali and Mubarak, 2017). However, estimating evapotranspiration (ET) often yields to high errors, particularly in arid and semi-arid regions (Gee and Hillel, 1988; Sukhija, 2003). Potential ET, which is what is most commonly estimated in the field, represents the greatest quantity of water that can be removed from a region via evaporation of transpiration (Ali and Mubarak, 2017). In addition to the climatic factors that influence potential ET, actual ET is also dependent on the unsaturated soil water storage and characteristics. This discrepancy can lead to frequent high errors in ET and recharge estimations (Freeze and Cherry, 1979). Recharge estimates based only on soil properties are also often incorrect as even small changes in the spatial variability can change the hydraulic parameters, which can have a significant effect on total infiltration (Freeze and Cherry, 1979; Nimmo, 2005).

Additional multi-scale heterogeneity from the connectivity and permeability of flow paths complicates the process of estimating recharge in fractured aquifers (de Dreuzy et al., 2002, 2004; Cook, 2003; Maréchal et al., 2004; Le Borgne et al., 2004, 2006; Jiménez-Martínez et al., 2013; Pedretti et al., 2016; Roques et al., 2018). Recharge in fractured aquifers typically travels by preferential flow path which can permit faster movement based on the characteristics of the

fractures and the present state of the system's hydraulics (Cook, 2003; Nimmo, 2005; Gleeson et al., 2009). Fractures permitting ample water can cause fractured-rock aquifers to recharge quickly during precipitation events or cause more extreme drawdown (Courtois et al., 2010). Recharge in fractured aquifers is also highly reliant on the dip of permeable structures and organization of the fractures (Gleeson et al., 2009; Ruelleu et al., 2010; Jiménez-Martínez et al., 2013; Leray et al., 2013). However, fully characterizing these flow paths is near impossible due to the depth and scale of the fractures as well as the variety in shape, orientation, and connectedness among other known and unknown characteristics (Nimmo, 2005; Gleeson et al., 2009). In addition, many traditional methods of quantifying recharge in aquifers are not directly applicable to fractured aquifers (Cook, 2003). Methods to characterize the local transmissivity of fracture networks include hydraulic tests (Day-Lewis et al., 2000), cross borehole flowmeter tests (Le Borgne et al., 2006), ground penetrating radar imaging (Day-Lewis et al., 2003), and tracer tests (Gleeson et al., 2009). These methods can be expensive, are often limited to local scale characterization, or invasive to the natural state of the groundwater system (Schuite et al., 2015). Also, the scale dependent nature of fractured aquifers reduces the reliability of short-term field studies as different aquifer features can control short term versus long term groundwater extraction (Jiménez-Martínez et al., 2013).

Recharge by fractures and dense fracture networks, such as fault zones, can also significantly aid in the recharge of groundwater systems (Ruelleu et al., 2010; Bense et al., 2013; Schuite et al., 2015). Localized flow can occur in the most conductive and connected fractures, which, as a result, causes the aquifer to be more responsive to recharge and pumping events (Courtois et al., 2010). The juxtaposition between the more permeable fractures and the less permeable crystalline matrix typically results in longer residence times for groundwater in these fractured-rock aquifer systems, particularly in the crystalline matrix (Farkas-Karay and Hajnal,

2015). However, these zones and paths of high permeability are limited by fracture extent and connectivity (Cook, 2003; Dewandel et al., 2012). Wide aperture fractures and the closely structured geology both have low storativity values; however, dense fracture networks, such as fault zones, can have high storativity, which can act as a recharge reservoir in groundwater aquifer systems (Bense et al., 2013). Deep fracture networks that have little connectivity to the surface can also recharge an aquifer, notably during dry periods and during long term pumping conditions (Roques et al., 2018).

Fractured Crystalline Aquifers

Crystalline aquifers, comprised of igneous and metamorphic bedrock, are commonly found throughout the world (Figure 1) (Maréchal et al., 2004; Gleeson et al., 2009; Pedretti et al., 2016; Dewandel et al., 2012; Maréchal et al., 2018); however, groundwater contained in crystalline bedrock is not always a dependable or sufficient water resource (Aquilina et al., 2004). Determining the reliability of each potential crystalline aquifer is imperative, as approximately one-third of the continental crust is composed of igneous and metamorphic rock (Blatt and Jones, 1975; Amiotte-Suchet et al., 2003; Gleeson et al., 2012). Despite their commonality, hydraulic properties of crystalline-rock aquifers are difficult to quantify due to their heterogeneous nature (Cook, 2003; Roques et al., 2016). With an average effective permeability from 10^{-15} to 10^{-17} m^2 (Freeze and Cherry, 1979; Gleeson et al., 2011; Stober and Butcher, 2014), metamorphosed and plutonic rocks have a close crystalline structure which results in a nearly impermeable structure with low primary porosity. Fractures within bedrock can provide ample pathways for water to flow through the system, potentially increasing the productivity these crystalline-rock aquifers up to four orders of magnitude (Kiraly, 1975; Clauser, 1992; Evans et al., 1997; Aquilina et al., 2004).

Based on the characteristics of the fracture conduit, water can favor a course of interconnected fractures through the aquifer, otherwise known as a preferential flow path (Cook, 2003; Nimmo, 2005; Gleeson et al., 2009; Pedretti et al., 2016; Roques et al., 2016; Ali and Mubarak, 2017; Schuite et al., 2017). If the geometry and hydraulic parameters of the fractured rock cannot produce sufficient discharge and therefore provide a significant through-flow system, it will generally not be considered an aquifer (Perdretti et al., 2016; Lamur et al., 2017).

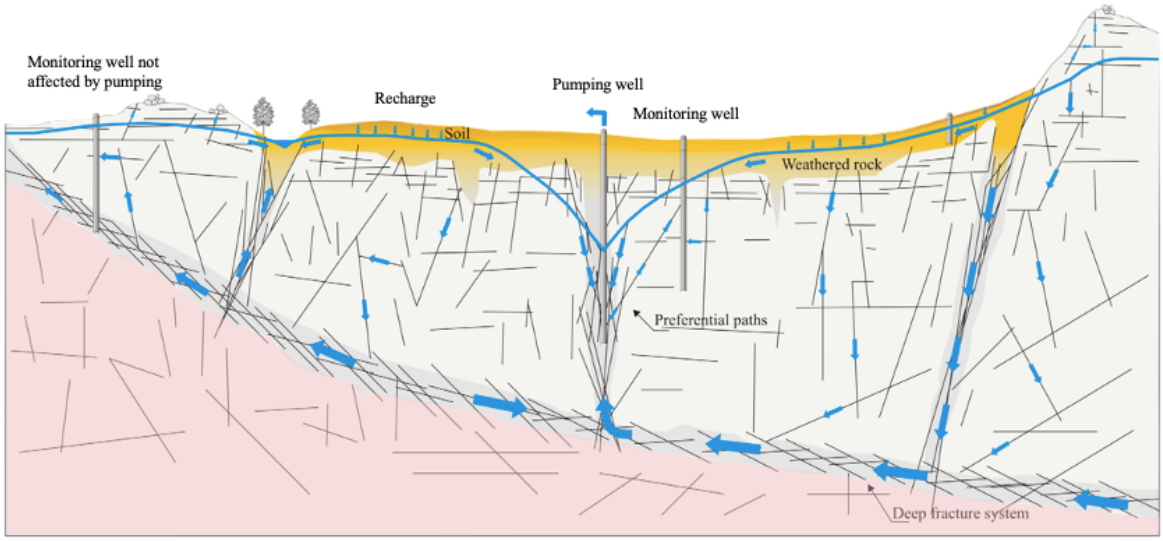

Figure 1: *Conceptual schematic of groundwater flow and recharge through the fractured crystalline-rock at the Ploemeur hydrogeologic site. Preferential flow paths, indicated with blue arrows, show where recharge and groundwater travels through the system. The deep fracture system, or the contact zone, shows larger blue arrows indicating more water traveling through the geologic feature. The pumping zone, located in the intersection of the contact zone and fault zones and shown by the pictured pumping well, contains multiple preferential flow paths for water to be extracted from the aquifer. The flow dynamics shown are simplified and do not fully represent the Ploemeur hydrogeologic site (Modified from Jiménez-Martínez et al., 2013)*

The unique hydraulic properties of each fractured crystalline-rock aquifer are dependent on factors such as the tectonic history, fracture connectivity, degree of weathering, stress history, climate, and elevation (Cook, 2003). A general hydrogeological model for fractured crystalline-rock aquifers has been used since the 1990s. Groundwater flow and aquifer properties are controlled by the weathering of the crystalline rock into mica-rich regolith and saprolite and weathered bedrock (Wright, 1992; Taylor and Howard, 1999). Typically, groundwater flow in crystalline aquifers occurs in the upper ~50 m where the bedrock has undergone sufficient weathering (Dewandel et al., 2012; Leray et al., 2013; Roques et al., 2016). A critical zone is defined at the bottom of the weathered bedrock and above the near-impervious unweathered bedrock where horizontal groundwater flow and transfer processes can be localized (Maréchal et al., 2018). Thus, process is important for understanding the hydraulic characteristics of the weathered saprolite and bedrock, particularly in this critical zone.

Groundwater travels through the weathered bedrock by small and enlarged fracture conduits, which can provide pathways for water to travel through. Primary fractures affect the small-scale permeability and porosity, while secondary fractures affect the geology at a larger scale (Maréchal et al., 2004). Deep basement plutonic and metamorphosed rocks are often not significantly weathered and are more affected by overburden stresses, resulting in structures that can be less effective at transporting water (Dewandel et al., 2012; Roques et al., 2016). Despite their low primary porosity, crystalline rocks tend to be prone to fracturing by brittle deformation, thus increasing their secondary porosities (Cook, 2003). The hydraulic properties of fractured crystalline-rock aquifers are scale dependent due to the variety of fracture densities and connected flow paths throughout the aquifer (Bour et al., 2002; Cook, 2003; Dewandel et al., 2012; Pedretti et al., 2016). To determine the connectivity of the fractures, researchers compare the ratios of

various fractures within the hydrogeologic system (Cook, 2003). Termination points, intersection points, end locations, alignments, locations, lengths, and densities are all significant fracture characteristics (Cook, 2003; Gleeson et al., 2009; Pedretti et al., 2016). However, determining the location and geometry of fractures in groundwater systems, particularly at depth, is near impossible due to their complicated geometry and multi-scaled connectedness (Nimmo, 2005). If large fractures or conduits allow water to travel through the system too quickly (e.g. karst systems), groundwater could undergo non-laminar flow, which is not accounted for in Darcy's Law (Darcy, 1856; Farkas-Karay et al., 2015). Fractures can also become clogged or have variable smoothness if small grains, such as weathered mica from crystalline bedrock become trapped in the fractures and conduits (Nimmo, 2005). Preferential flow paths can create localized productive flow, but a crystalline-rock aquifer may not yield enough water even if the fractures are not well connected or if the wells are not drilled in the optimal locations (Kiraly, 1975; de Dreuzy et al., 2002; Courtois et al., 2010; Roques et al., 2016).

Tectonic activity can create fractures and conduits in the close crystalline structures found in hard rock aquifers (Bense et al., 2013; Roques et al., 2016). Fault zones, which occur when fault-driven deformation affects the permeability of rock, are often found in tectonically altered regions (Bense et al., 2013). Structural features of the fault, such as the thickness, root depth, and dip angle, as well as the remote stresses, displacement, and age impact the storage and ability of water to travel through the system (Caine et al., 1996; Bense et al., 2013; Roques et al., 2014, 2016); however, the properties of a fault zone can be highly variable locally, both at the watershed scale, and the regional scale (Caine et al., 1996; Bense et al., 2013; Roques et al., 2014, 2016). Hydraulic gradients surrounding fault zones are influenced by a variety of factors including topography, groundwater extraction, and sediment compaction (Bense et al., 2013). Many

crystalline rock aquifers contain small sheer zones, which can produce limited groundwater resources of a few cubic meters per hour and are consequently useful only at a local scale, typically for sole domestic use (Taylor and Howard, 1999; Dewandel et al., 2006; Roques et al., 2016). However, major geologic structures such as large fault zones and regional contact zones can produce high groundwater yields in crystalline-rock aquifers through increased permeability of between two to three orders of magnitude (Evans et al., 1997; Bense et al., 2013; Roques et al., 2016). Vertical and sub-vertical fault zones and contact zones can contribute to the productivity of wells in a groundwater system, but they generally possess relatively low storage and exhibit a small surface area, thus limiting the quantity of direct recharge (Figure 2a) (Leray et al., 2012; Roques et al., 2014, 2016). Vertical and subvertical fault zones can also act as impervious boundaries to flow perpendicular to the strike of the fault (Caine et al., 1996; Seaton and Burbey, 2005; Rugh and Burbey, 2008; Gleeson et al., 2009; Roques et al., 2016). Horizontal and sub-horizontal structures are able to collect more recharge leading to increased radial flow due to their larger surface areas for catchment (Figure 2b) (Cook, 2003; Ruelleu et al., 2010; Leray et al., 2013; Roques et al., 2016), while a gentle dip can contribute to the yield of the structural feature as groundwater tends to follow topography (Seaton and Burbey, 2005; Le Borgne et al., 2006; Ruelleu et al., 2010; Leray et al., 2013). Fault zones connected to an overlaying reservoir prove to be the most productive framework for sustained long-term groundwater pumping (Ruelleu et al., 2010; Leray et al., 2013; Roques et al., 2014, 2016). Fault zones in crystalline rock aquifers can potentially greatly enhance well productivity, but characterizing fault zones, in particular sub-horizontal zones at depth, is difficult and expensive using current conventional methods (Roques et al., 2016).

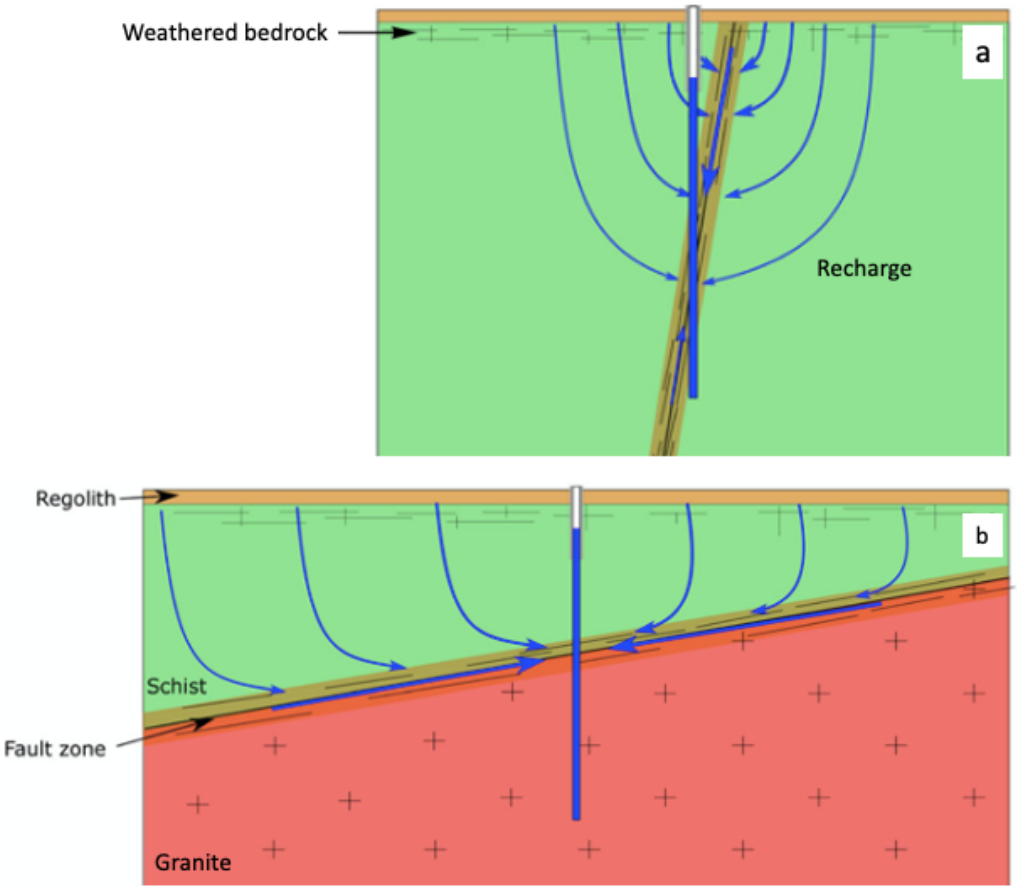

Figure 2: *Recharge traveling from the ground surface into a subvertical fault zone and a sub-horizontal fault zone. Subvertical fault zones* ***(a.)*** *can contribute to the productivity of an aquifer, but they often have smaller surface areas and limited storage. The large surface area of a sub-horizontal unit* ***(b.)****, including fault zones and contact zones, often improves aquifer productivity due its ability to collect more recharge (Modified from Roques et al., 2016).*

Flow through the Vadose Zone

The vadose zone, sometimes referred to as the unsaturated or aeration zone, is the hydrological connection between land surface and the water table (Bouwer, 1978, Freeze and Cherry, 1979; Haverkamp et al., 1999; Nimmo, 2005). Recharge of groundwater reservoirs and aquifers typically occurs through the vadose zone (Haverkamp et al., 1999). The vadose zone has natural heterogeneity from the hydraulic properties of soil, rocks, and organic matter as well as the

added complexity of vegetation (roots) and climate. The heterogeneity is scale dependent on micro, watershed, and regional scales. Water in the vadose zone is influenced by unsaturated hydrostatics, such as volumetric water content, energy, capillary pressure, and soil water retention, and hydrodynamics, such as hydraulic diffusivity and preferential flow. The flow processes occurring in the vadose zone affect a variety of hydrologic processes in groundwater aquifer systems (Nimmo, 2005). Because of the scale dependent complexity in the vadose zone, we must work to understand the hydraulic interactions to better estimate the rates, timing, and flow patterns of recharge in groundwater aquifer systems.

The vadose zone is separated into three sections: the upper root zone, the intermediate zone, and the capillary fringe. Depending on the regional climate, the root zone is typically a few meters in thickness, defined by the depth of plant roots (Guymon, 1994; Hornberger et al., 1998). The intermediate zone separates the upper root zone and the lower capillary fringe, and it varies in thickness depending on the regional climate and geology and the depth of the saturated zone. The saturated capillary fringe lies just above the water table where the capillary forces, dependent on the hydraulic interactions between water and the matrix, suction groundwater upward from the water table (Haverkamp et al., 1999; Nimmo, 2005). The thickness of the capillary fringe is inversely proportional to the grain size at the water table elevation, with small grain sizes having thicker capillary zones and vice versa (Tolman, 1937; Guymon, 1994; Nimmo, 2005).

Key hydraulic exchanges occur between the subsurface, surface water, and the atmosphere in the vadose zone. Water from precipitation and surface water infiltrates the soil through the surface. The physical process of infiltration depends on the whether the recharge was ponding on the surface as a boundary condition or whether the recharge acted as a flux from rainfall (Haverkamp et al., 1999). As recharge percolates through the vadose zone, it loses water to the

water table (groundwater recharge) through evaporation, ET, and drainage (Haverkamp et al., 1999; Ali and Mubarak, 2017). The rate of infiltration through the unsaturated zone decreases with time to a constant rate because the water capacity of the zone fills as recharge water accumulates (Freeze and Cherry, 1979). ET removes water from the vadose zone based on the soil moisture, atmospheric conditions, and vegetation type and density. The amount of water uptake is limited by the atmospheric conditions; however, in drier seasons, the water uptake decreases, even in the same atmospheric conditions, to help regulate the flow of water to plant roots (Horenberger et al., 1998).

The unsaturated flow theory examines two types of factors when determining water movement: driving forces, such as gravity and matrix pressure, and properties of the medium, including water retention and hydraulic conductivity (Nimmo, 2005; Ali and Mubarak, 2017). Additionally, the volumetric moisture content (θ), defined as $\frac{Volume\ of\ Water\ (Vw)}{Total\ Volume\ (Vt)}$, plays an essential role in vadose flow (Nimmo, 2005). In unsaturated flow above the capillary fringe, the volumetric moisture content is less than the porosity (n). The total volume (V_t) is the complete unit volume of a soil or rock and includes the volume of solids (V_s), water (V_w), and air (V_a) (Freeze and Cherry, 1979).

Water travelling through unsaturated porous media is treated as one-dimensional vertical flow and is defined by the continuity equation:

$$\frac{\partial \theta}{\partial t} = \frac{\partial q}{\partial z} \tag{1}$$

where θ is the volumetric soil water content, q is water flux, z is depth positive in the downward direction, and t is time (Buckingham, 1907; Haverkamp et al., 1999; Nimmo, 2005). This can be combined with Darcy's Law (Darcy, 1856), which states that flux (q) is proportional to the driving force of flow, or the hydraulic gradient ($\frac{\partial H}{\partial z}$),

$$q = -K(\theta)\frac{\partial H}{\partial z} \quad (2)$$

where H is defined as hydraulic head, or the energy of soil water per unit weight at a given depth and K is the hydraulic conductivity of the soil as a function of θ (Darcy, 1856; Nimmo, 2005; Ali and Mubarak, 2017). The continuity equation (1) combined with Darcy's Law (2) can be simplified as:

$$\frac{\partial \theta}{\partial t} = \frac{\partial}{\partial z}[\, K(\theta)(\frac{\partial h}{\partial z} - 1)] \quad (3)$$

where h is the pressure head in the soil relative to atmospheric pressure ($h \leq 0$) (Haverkamp et al., 1999). An alternate form of unsteady or transient vadose flow that depends on hydraulic diffusivity is based around a variation of Richards' (1931) equation, yielding:

$$\frac{\partial \theta}{\partial t} = \frac{\partial}{\partial z}[\, D(\theta)\frac{\partial}{\partial z}(\theta)\,] \quad (4)$$

where $D(\theta)$ is diffusivity, a material property dependent on soil water content, which can be easier to measure and less variable than $K(\theta)$ in unsaturated conditions. This equation requires the assumption that flow is driven by water content gradients, as opposed to potential energy (Childs and Collis-George, 1950; Nimmo, 2005).

Hydrogeologic Study Site

The Ploemeur hydrogeologic site, located 15 km from the southeastern coast of Brittany, France, has provided groundwater to over 20,000 residents in the town of Ploemeur for nearly 30 years (Figure 3). A quarter of the Brittany's drinking water originates from groundwater resources, from which 40% comes from crystalline aquifers (Roques et al., 2016). The Ploemeur aquifer is considered prolific for a crystalline-rock aquifer with high yields of 1 million m^3 per year, over four times larger than the average crystalline-rock aquifer (Mougin et al., 2008; Roques et al.,

2016). A productive groundwater resource in French Brittany is important as the top 30 m of soil and bedrock in the region is susceptible to contaminants from agriculture (Aquilina et al., 2012). Over 180 wells have been drilled in this aquifer for groundwater measurements and monitoring since the mid-1990s (Schuite et al., 2015). The elevation in the region is near sea level reaching no more than 50 m in elevation. The study site has an oceanic climate, with an average annual precipitation of 900 mm and mean annual recharge of 260 mm (Leray et al., 2012, Jiménez-Martínez et al., 2013; Roques et al., 2018). Located within the Armorican Massif, the Ploemeur hydrogeologic site is made up of Hercynian mica-schist overlying upper-Carboniferous syntectonic leucogranite intrusions (Touchard, 1999; Roques et al., 2016). Separating the two bedrock units is a north dipping, sub-horizontal contact zone composed of mica-schist intruded by granite spanning 10 to 100 m in thickness (Figure 4) (Touchard, 1999; Le Borgne et al., 2006; Ruelleu et al., 2010). The regional bedrock is heavily faulted with NNW-SSE faults from the Hercynian orogeny, and the hydrogeological study site has a crosscutting subvertical, dextral normal fault striking N20°E (Touchard, 1999; Roques et al., 2016).

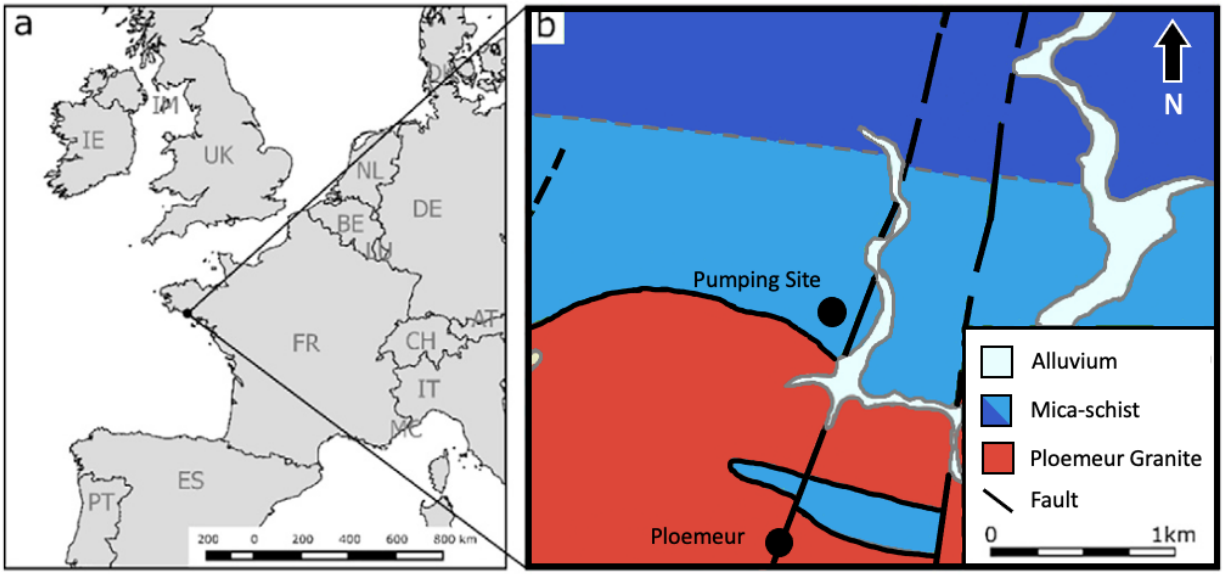

Figure 3: *Geographic location* ***(a.)*** *and geologic map of the Ploemeur hydrogeologic site* ***(b.)*** *in Brittany, France. (Modified from Aquilina et al., 2018).*

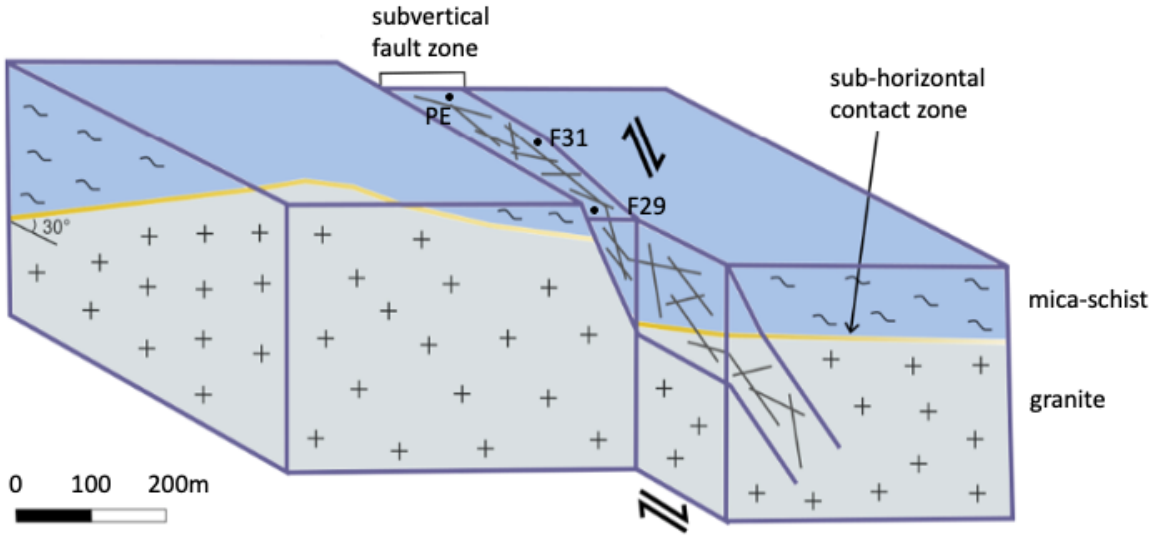

Figure 4: *Conceptual block diagram of the geologic units and structures at the Ploemeur hydrogeologic site. The contact zone (yellow) lies between the Ploemeur granite (grey +) and mica-schist (blue ~). The subvertical normal fault and surrounding fault zone are represented between the two blocks to show the tectonic movement at the site. The locations of the three pumping wells, PE, F31, and F29, are shown. (modified from Schuite et al., 2015).*

Both the mica-schist and granite units contain significant fractures from Silurian and Devonian techno-metamorphic events (Roques et al., 2018). The mica-schist exhibits ductile deformation from the granitic intrusions with increased fracture intensity toward the contact zone (Le Borgne et al., 2006). The Ploemeur granite extends to a depth of up to one kilometer deep (Vigneresse, 1983) and is composed of quartz, K-feldspar, plagioclase, muscovite, and biotite (Roques et al., 2018). Due to its depth, the granite is less weathered than the overlying layers, and it is locally permeable (Touchard, 1999; Dewandel et al., 2012). The cross-cutting fault spans 50 to 150 m in width (Touchard, 1999). Both the fault and the contact zone exhibit high hydraulic conductivity values relative to the surrounding crystalline bedrock. The contact zone has been

found to be twice as transmissive as the fault zone, but the fault zone has 2 to 7 times more storage than the contact zone which is likely from the intensity of fracturing in the fault zone (Le Borgne et al., 2006).

Overlying the mica-schist is a layer of weathered regolith 10-30 meters in thickness, with increased weathering near the contact zone. Due to the presence of mica in the bedrock, the regolith has a clay-like structure which provides ample storage but can impede flow (Dewandel et al., 2012; Roques et al., 2018). This characteristic causes water to pool on the surface prior to pumping conditions (Roques et al., 2018). The Ploemeur multiscale complex heterogeneities and localized flow paths occur primarily through this weathered regolith (Le Borgne et al., 2006; Jiménez-Marténez et al., 2013; Aquilina et al., 2015; Roques et al., 2018), causing a nearly two-month lag between precipitation events and water-table response in bedrock wells (Law, 2019). The general flow path in the regolith is from the higher elevations in the northwest part of the study area to the lower elevations of the southeast (Aquilina et al., 2015; Roques et al., 2018).

The Ploemeur hydrogeological site has been monitored since its discovery in 1991, when it became part of the H+ hydrogeological network of the University of Rennes. Nearly 50 wells, ranging from 30 to 150 m in depth are monitored and three are used as domestic pumping wells (Roques et al., 2018). The intersection between the fault zone and subvertical contact zone has been the most productive in terms of groundwater extraction (Touchard, 1999; Le Borgne et al., 2006). Wells drilled into the bedrock are not prolific (Touchard, 1999). Since 2001, the three pumping wells in the intersection of the contact zone and fault zone produce 1 million cubic meters of groundwater per year, or 2.66×10^6 L daily (Touchard, 1999; Le Borgne et al., 2004). The aquifer underwent 20 m of drawdown during the first 6 years of pumping, but the water levels have remained steady ever since (Roques et al., 2018). Despite the relatively low levels of drawdown,

the pumping site exhibits a radius of influence of over 600 m (Le Borgne et al., 2006). The amount of water produced by the region and the radius of influence from pumping indicate that features beyond just the sub-horizontal contact zone are influencing the quantity of drawdown near the extraction wells (Ruelleu et al., 2010).

The groundwater system at the site prior to pumping had an upward flux, which produced natural surface discharge observed in artesian wells at the site (Le Borgne et al., 2004; Jiménez-Martínez et al., 2013). Water extracted from the system originates from both shallow and deep sources within the aquifer, with deeper water dominating the system after five years of pumping (Aquilina et al., 2015; Roques et al., 2018). Ayraud et al. (2008) found that modern water (< 50 years) dominates the shallow storage at the Ploemeur hydrogeologic site. However, deeper regional flow with longer residence times (> 50 years) has been identified in the contact zone and along the fault trace (Aquilina et al., 2015). Roques et al., (2018) also observes that water extracted from the aquifer represents a mixture between older (40+ years) and newer (0-40 years) water with an average groundwater age between 20 and 40 years, with age increasing with depth. Deeper fractures and groundwater flow paths in the aquifer system have average residence times of 50+ years, and the shallower fractures in the top 30 meters of the aquifer have a residence time of up to 30 years (Leray et al., 2012; Aquilina et al., 2015; Roques et al., 2018). Therefore, recharge is controlled by the shallow bedrock fractures, fault zone, as well as the sub-horizontal contact zone. Such residence times are variable through the system due to the intrinsic heterogeneity of fractured and faulted crystalline-rocks (Roques et al., 2018). The unique geometry of the regional faults and permeable sub-horizontal contact zone allows for these substantial water yields from the Ploemeur aquifer.

MODEL

Conceptual Model

We use a three-dimensional regional numerical model to simulate the flow paths of recharge and extracted groundwater during the average pumping conditions at the Ploemeur hydrogeologic site. The goal of the model is to determine the source of the groundwater extracted from the pumping wells during the first years of pumping conditions by simulating the 10-year average recharge and pumping conditions. We do not seek a perfect match between the field observations and the model results; instead, we want to understand the temporal trends and hydromechanics of the hydrogeology in order to better understand the general functioning of this complex system. This study will help us understand which geologic units contribute the most water to the pumping well and what units recharge prefers to travel through. In addition, this study contributes to the process of understanding the impact of hydromechanical properties within the Ploemeur aquifer system, which can be used to understand fractured and faulted crystalline-rock aquifers worldwide.

The Ploemeur hydrogeologic site and model covers an area of slightly less than 1000 km^2, which is typical of small watersheds (Leray et al., 2013; Schuite et al., 2017). The model elevation spans from 50 m above sea level western side of the area to 20 m just east of the pumping wells (Figure 5). The main geologic features observed at the Ploemeur hydrogeologic site and represented in the model include the mica-schist, granite, contact zone, fault zone, and regolith units. Initial ranges for hydraulic parameters are obtained from field observations (Le Borgne et al., 2006) and previously calibrated models of the region (Table 1) (Leray et al., 2012). A confined aquifer model represents the Ploemeur aquifer system best due to the abundance of clay-like minerals in the micaschist (Le Borgne et al., 2006; Leray et al., 2012; Jiménez-Martínez et al.,

2013; Schuite et al., 2015). The heterogeneity and localized flow found in fractured crystalline-rock aquifers pushes the limitations of classical methods of groundwater modeling (Cook, 2003; Maréchal et al., 2018). To account for this complexity, we use the multizone approach characterizing the geologic units by equivalent porous geometric zones with representative, unique, scale-independent hydraulic parameters (Day-Lewis et al., 2000; Cook, 2003; Schuite et al., 2017). This allows us to mimic the unique geometric zones of the region, such as the fault zone and contact zone, while utilizing the traditional groundwater flow equations with MODFLOW (Le Borgne et al., 2004; Cook, 2003). In addition, dense fracture networks such as fault zones, are represented as homogenous features since our model does not account for individual unit heterogeneity (Bense et al., 2013; Schuite et al., 2017). Therefore, our model does not fully represent the effects of the heterogeneities expected to be found within the individual units of the Ploemeur hydrogeologic site.

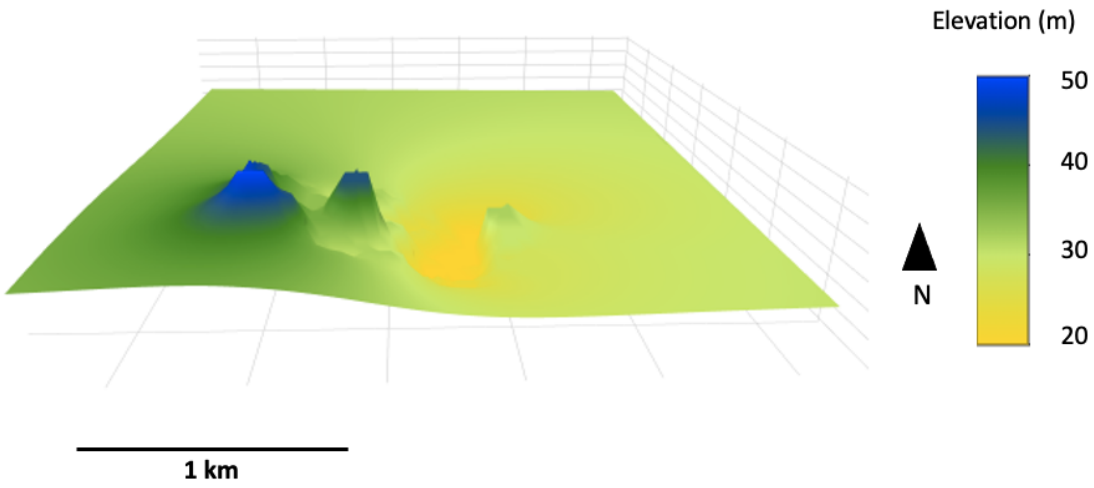

Figure 5: *Digital elevation model of the simulated elevation at the Ploemeur hydrogeologic site. The highest elevation at 50 m is shown in blue, and the lowest elevation at 20 m is shown in yellow. More detailed elevation data is shown in the southern central region of the figure, which is the location of the pumping site. The surrounding elevation is interpolated based on the elevation at the pumping site. Figure made in RStudio (RStudio Team, 2020).*

	K_x (m/d)	K_z (m/d)	S_s (1/m)	Porosity
Regolith	6.57	0.65	2.00×10^{-3}	0.1
Mica-schist	1.0×10^{-4}	8.62×10^{-2}	1.00×10^{-5}	0.05
Contact zone	86.4	8.6	1.00×10^{-3}	0.1
Ploemeur granite	8.64×10^{-7}	8.64×10^{-8}	1.00×10^{-6}	0.05 – 0.01
Fault zone	1.08	0.108	1.20×10^{-2}	0.1

Table 1: *The hydraulic parameter estimates for the geologic units and features at the Ploemeur hydrogeologic site based on field observations from Le Borgne et al. (2006) and model results from Leray et al. (2012). These parameter estimates of horizontal hydraulic conductivity, vertical hydraulic conductivity, specific storage, and porosity are used as model inputs to the numerical model. The porosity in the granite varies with depth where the granite units closer to the land surface have the higher porosity of 0.05, and the deeper granite units have a lower porosity of 0.01. This assumes that the granite contains more fractures closer to the land surface and vice versa.*

The topmost 20 meters is simulated to represent soil and weathered mica-schist regolith, which together are treated as part of the variably saturated vadose zone (Figure 6). Below the regolith is the mica-schist bedrock, which varies in thickness depending on spatial location. The contact zone, modeled with a thickness varying from 10 m at the surface to 30 m at depth, separates the micaschist and granite bedrock. The modeled granite layer reaches a depth of 300 m below sea level (the base of the model). The contact zone, which dips 30° from the surface to a depth of 250 m, reaches the surface on either side of the pumping zone. Cross-cutting the model area from the northeast to southwest is the fault zone modeled to be 100 to 150 m wide based on field observations (Touchard, 1999; Le Borgne et al., 2004). Both the northern and southern borders of the model area are simulated as general-head boundaries in the saprolite, contact zone, and fault

zone as there are no known boundary features exist to inhibit flow from traveling toward or away from the pumping zone through these features. The general-head boundaries are equal to the initial head values at the site. No general-head boundaries are applied in the mica-schist or granite units due to their lower values of permeability and assumed minimal exchange of groundwater through these units across the model boundary. The eastern and western borders of the model area are represented as no-flow boundaries, as these regions have additional cross-cutting faults on either side of the modeled area, which are believed to inhibit later flow. The model base is also represented as a no-flow boundary as the hydraulic properties of the Ploemeur granite limit the amount of vertical flow across the base. Nine observation wells and three pumping wells (F31, PE, and F29) are utilized in this study. In total, the pumping wells extract 2800 m^3/d from the site to yield 1 million m^3/year, and they reach depths up to 90 m below the land surface. All of the pumping wells are located at the intersection of the fault zone and the contact zone, which varies between 30 to 150 m in depth depending on their spatial location. The initial head values in the model are defined to be 10 m below the surface elevation. The pumping wells are located near the region with the lowest elevation at ~20 m. The model simulates the beginning of pumping conditions, beginning in 1991, when monitoring at the site commenced.

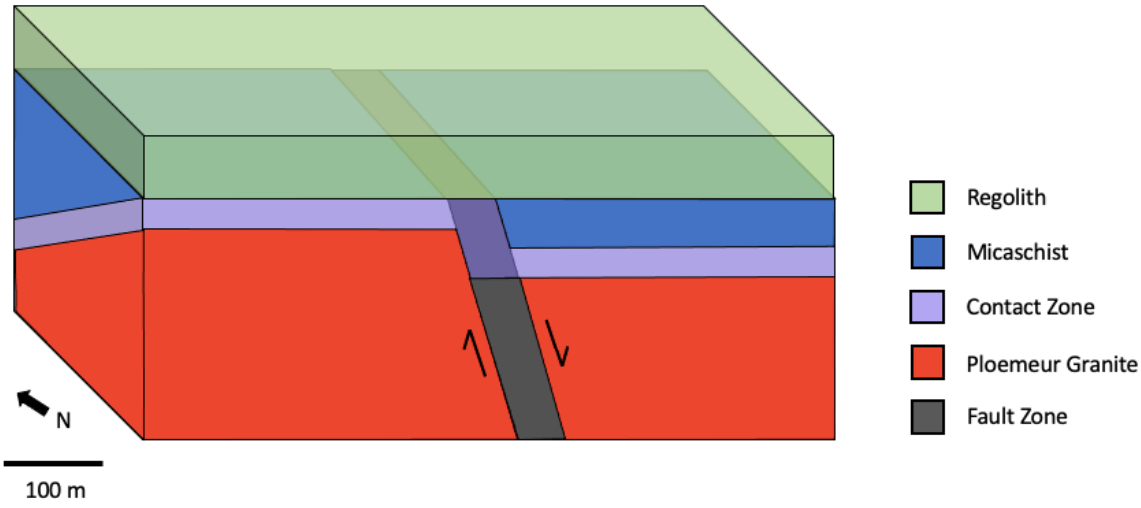

Figure 6: *Simplified block diagram of the conceptual model for the Ploemeur hydrogeological site showing the geologic units as equivalent porous media geometric shapes (Modified from Le Borgne et al., 2006).*

Despite relatively low rates of infiltration at the study area during the summer months, we show recharge infiltrating the system year round with average annual recharge estimates for the Ploemeur hydrogeological site ranging between 304-307 mm per year (Law, 2019). Law (2019) averaged the monthly recharge based on field and climate observations for a 25 year period and repeated the average monthly recharge and infiltration estimates each year. This estimate is greater than previously published estimates due to the addition of analyzing recharge traveling through the unsaturated zone, which has not been previously investigated. Based on the recharge estimates from Law (2019), an approximate area of 0.8 km would theoretically be required to supply enough recharge for the drawdown and pumping conditions. However, this areal estimate assumes that all recharge simulated within the area of our model supplies the groundwater extraction from the pumping wells, and that said recharge reaches the pumping well almost immediately. Thus, this neglects the role of storage and potential flow mechanisms involving storage and piston-flow

concepts. Because of said uncertainties and assumptions, our model area is approximately 11 times larger than that estimated areal requirement. The larger area accounts for the regional recharge catchment between the closest groundwater divides to the East and West (Leray et al., 2012) as well as the impact from higher elevation regions west of the pumping zone.

MODFLOW Model

For our transient model of the Ploemeur hydrogeologic site, we use MODFLOW 6 (Langevin et al., 2021) along with the graphical user interface ModelMuse v. 4.3.0.0. (Beta Version 6) (Winston, 2020), both developed by the U.S. Geological Survey (USGS). MODFLOW utilizes a finite difference method that divides the grid representing the aquifer system into cells of a user-specified size with user-specified hydraulic parameters. Our model is composed of 60 rows and 65 columns with a cell size of 50 by 50 m spanning a spatial distance of 3 km in the east-west direction, 3.25 km in the north-south direction, and 350 m vertically (50 m above sea level and 300 m below the land surface). Initially, a forward modeling process is implemented that utilizes literature estimates of hydraulic properties as input parameters to simulate the resulting hydraulic head values for each model cell. The geologic units at the hydrogeologic site (regolith, mica-schist, contact zone, and granite) are defined as layers in the model, and polygon objects define the hydraulic parameters for each layer and are set with the z-coordinates, or elevations, of the layers. The mica-schist, granite, and contact zone are each defined with five layers, and the regolith is defined with one layer. The fault zone is defined solely as a polygon object. The locations of the wells and topographic contours around the pumping site were imported from a GIS shapefile. We use the imported elevation data to interpolate surface elevations across the hydrogeologic site. Geologic units and features in the model with changing z-elevations, such as

the contact zone, are defined with interpolation objects set across the model area to mimic the geologic complexity of the hydrogeologic site.

The IMS (Iterative Model Solution) Package is used to solve the nonlinear set of finite-difference equations. The package parameters were altered to encourage convergence and accommodate the complexity of the model. The complexity input in the IMS Package is set to MODERATE, which encourages model convergence and allows the model to run to completion. Additionally, we alter nonlinear IMS parameters, including the Outer HClose, the under-relaxation scheme, the under-relaxation theta, and the under-relaxation kappa to be consistent with the recommended values for SIMPLE or MODERATE complexity models (Winston, 2019). The delta-bar-delta (DBD) relaxation scheme is used to increase the solution's stability and improve model convergence (Smith, 1993; Hughes et al., 2017). We use the MAW (Multi-Aquifer Well) Package for the pumping wells to account for the variations in permeability between the contact zone, mica-schist, and granite. The GHB (General-Head Boundary) Package is used to simulate inflow or outflow along the northern and southern borders to represent no impedance of flow to regions outside the model domain where no known physical barriers exist. Specifically, the general-head boundaries are set in the weathered mica-schist regolith on both the northern and southern boundaries in addition to the contact zone layers and fault zone along the northern boundary (Table 2). These areas represent the primary potential pathways for water flow into the model due to their hydrogeologic permeabilities and geometries (Touchard, 1999; Le Borgne et al., 2006; Ruelleu et al., 2009). The boundary heads of the GHBs are based on the interpreted initial head values at the locations of the model boundaries.

	Northern Boundary		Southern Boundary	
	K_x (m/d)	Conductance	K_x (m/d)	Conductance
Regolith	6.57	0.032	6.57	0.032
Contact zone	86.4	2.88	-	-
Fault zone	1.08	0.002	1.08	0.002

Table 2: *Input parameters for the general-head boundaries (GHBs) on the northern and southern borders of the model area. The boundary head values are set to the initial head values at the locations of the boundaries varying from 14 to 26 m on the northern boundary and 18 to 40 m on the southern boundary. The conductance values are calculated with the equation K/M and the Conductance Interpretation is set to Calculated for the Polygon Objects. The contact zone does not exist along the southern border because it reaches the model surface north of the southern boundary. The GHBs are set across the whole boundary for the regolith and contact zone and are set for the object width in the fault zone.*

We use the UZF6 (Unsaturated Zone Flow) Package for MODFLOW 6 in the weathered regolith layer to simulate the storage and recharge of the variably saturated zone (Niswonger, 2006). Simulating the flow through the vadose zone allows us to identify how the zone influences the quantity and timing of recharge infiltration entering the groundwater system. The UZF Package utilizes a kinematic wave approximation to Richards' equation, which is solved using the method of characteristics. Richards' equation (1931) is simplified in the UZF Package to:

$$\frac{\partial \theta}{\partial t} = \frac{\partial}{\partial z}[\mathrm{D}(\theta)\frac{\partial \theta}{\partial z} - K(\theta)] - i \tag{5}$$

where

θ is volumetric water content

q is water flux [L/T]

z is vertical depth [L]

$D(\theta)$ is hydraulic diffusivity [L^2/T]

$K(\theta)$ is unsaturated hydraulic conductivity as a function of water content [L^2/T]

i is ET rate per unit of depth [L^2/T]

t is time [T],

which shows the vertical movement of the unsaturated flow (Langevin et al., 2017).

The approximation method used in the UZF Package assumes that the gravitational forces represent the only driving force of vertical flux, thus removing the diffusivity term from the equation (Ali and Mubarak, 2017). The method also assumes that evaporation is immediately removed from the soil column and that all flow travels vertically downward (Figure 7). Incorporating these assumptions leads to the final form of the Richards' equation (Equation 5) as:

$$\frac{\partial \theta}{\partial t} + \frac{\partial K(\theta)}{\partial z} + i = 0 \tag{6}$$

Water traveling through the vadose zone occurs in drying and wetting fronts, or waves where an increase in infiltration causes a wetting front and vice versa. We rewrite Equation 6 as a partial derivative of θ with respect to t and z to examine the wave of the wetting front:

$$\frac{\partial \theta}{\partial t} + \frac{\partial K(\theta)}{\partial z}\frac{\partial \theta}{\partial z} = -i \tag{7}$$

We combine Equation 7 with Abbott's equation of variation (1966) to yield:

$$\frac{\partial \theta}{\partial t}dt + \frac{\partial \theta}{\partial z}dz = d\theta \tag{8}$$

which can be written in matrix form as:

$$\begin{bmatrix} 1 & \frac{\partial K(\theta)}{\partial \theta} \\ dt & dt \end{bmatrix} \begin{bmatrix} \frac{\partial \theta}{\partial t} \\ \frac{\partial \theta}{\partial z} \end{bmatrix} = \begin{bmatrix} i \\ d\theta \end{bmatrix} \tag{9}$$

and then expanded into its determinants:

$$\frac{\partial z}{\partial t} = \frac{\partial K(\theta)}{\partial \theta} = v(\theta) \tag{10a}$$

$$\frac{\partial \theta}{\partial t} = -i \tag{10b}$$

$$\frac{\partial \theta}{\partial z} = \frac{-i}{v(\theta)} \tag{10c}$$

where Equation 10a represents the velocity of the wave in the unsaturated zone, 10b represents the change in the water content of the wave over time, and 10c represents the change in water content with vertical distance following the wave. The UZF Package calculates the shortest time of any two waves to intersect during the model simulation (Langevin et al., 2017).

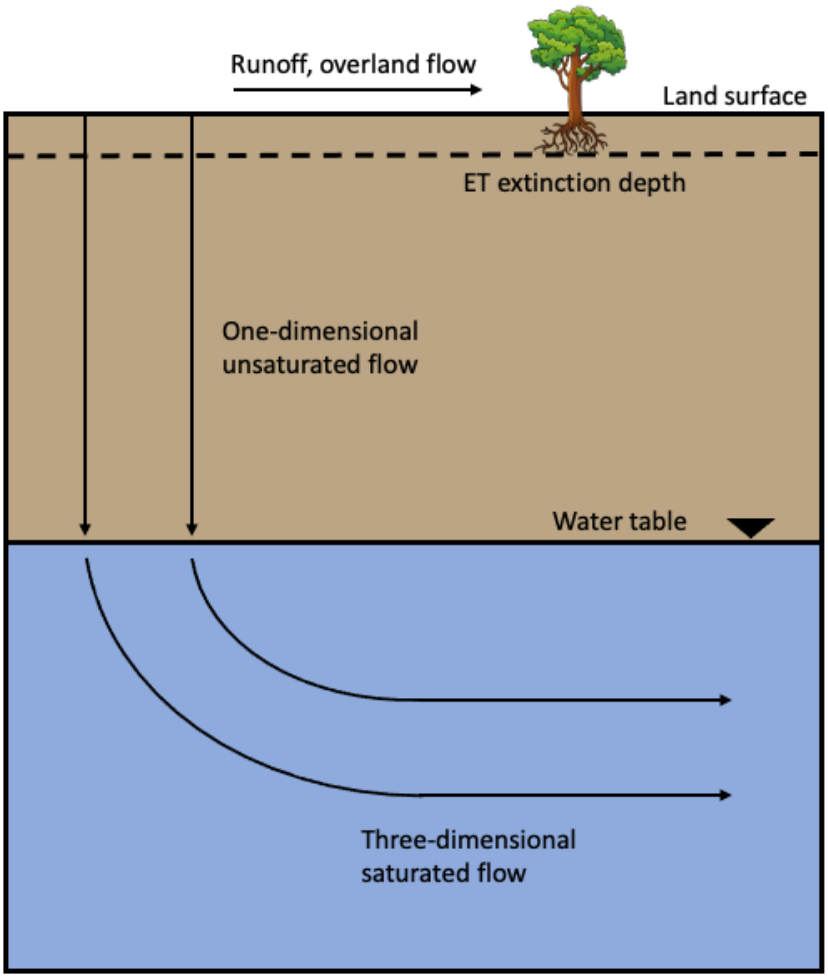

Figure 7: *A simplified conceptual diagram showing recharge traveling through a groundwater system to the aquifer. We see vertical flow through the vadose zone and horizontal flow in the saturated zone, which is an assumption driving the UZF Package. The diagram also shows the evapotranspiration extinction depth at the root extinction depth (Modified from Niswonger et al., 2006).*

We utilize the UZF Package because it simulates the observed (or estimated) infiltration rate to the model surface and removes the evapotranspiration (ET) first from the unsaturated zone and then from the groundwater reservoir. This varies from the Recharge (RCH) and Evapotranspiration (EVT) Packages available in MODFLOW as these packages apply the recharge directly to the water table and removes water via ET as a function of the extinction depth prior to adding it to the groundwater reservoir if the water demand is not met (Harbaugh, 2005; Niswonger

et al., 2006). The UZF Package simulates the recharge and ET as a variable thick plane over the three-dimensional saturated zone model. The thickness of the unsaturated zone is determined by calculating the difference between the user-specified land elevation data at each cell and the model calculated hydraulic head to determine the thickness of the unsaturated zone within each cell. The package then estimates the mass balance from the residual water content by calculating specific retention as specific yield and subtracting it from the saturated water content. Water discharged to the surface is removed from the model area through the pumping wells or GHBs. The model incorporates the evapotranspiration and infiltration data averaged over 25 years from Law (2019) in the UZF Package. Previous studies calculated an extinction depth of 3 m below the land surface and a water content of 0.13 (Leray et al., 2012; Jiménez-Martínez et al., 2013). These values are used in this model.

We also implement post-processing packages, including Zonebudget for MODFLOW 6 (ZONBUD) and MODPATH v. 7.2.01 (Harbaugh, 1990; Pollock, 2017). Zonebudget determines the quantity of water flowing between each geologic unit found in the Ploemeur hydrogeologic site using subregional water budgets (Harbaugh, 1990). Five zones are used to represent the geologic units in the model: granite, mica-schist, regolith, fault zone, and contact zone. Zonebudget also determines the inflows and outflows from each unit using additional packages such as the pumping wells (MAW Package) and the northern and southern boundaries (GHB Package). We use MODPATH to track water as particles traveling through the system (Pollock, 2017). Both backward and forward tracking are used to determine the pathways of water travelling to and from the pumping wells. Backward tracking shows were water in a selected location originates from, and the simulation occurs during infinite time. A time series analysis in backward tracking estimates the distances the water particles travel during the simulated model time.

Forward tracking shows where water particles travel after being placed at a user-specified location. Forward tracking can only show particle motions occurring during the length of the model simulation.

The model simulates the first six years of pumping conditions with each day simulated as a time step providing 2190 time steps with each year having 365 daily time steps. An initial time step is calculated in steady state conditions, and then the remaining 2190 time steps are solved as transient conditions. The temporal model inputs, including recharge, infiltration, and hydraulic head observations, are represented as long-term monthly averages. Law (2019) calculated the monthly recharge estimates using the average recharge estimates for each month for up to 25 years to account the variations in seasonality between the summer months and rainier winter months over a 25 year period beginning in 1991, thus providing results that are accurate in the long term (Jiménez-Martínez et al., 2013).

Model Calibration

We use ModelMuse 4 for MODFLOW with PEST capabilities to calibrate the hydraulic parameters of the model using head observations from monitoring wells surrounding the pumping zone (Doherty, 2015; Winston, 2020; Under Beta Testing). We incorporate the hydraulic head observations from nine monitoring wells using the Observation (OBS) Package to calibrate the model. To be consistent with our recharge data inputs, we take the average head values for each month over the first 10 years of pumping conditions at each monitoring well (Table 3). Pumping at the Ploemeur hydrogeologic site began at the beginning of 1991, but the first observational data is from April 1991. Not all of the recorded monitoring wells have data from the beginning of pumping conditions, so we include the average monthly data for the subsequent 10 years at that

monitoring well from the date the recorded data commences. The number of head observations at the monitoring wells recorded each month is not consistent from month to month or from well to well. Taking the average monthly values over 10 years will not show the higher frequency changes in head values of each individual year, but rather will show the long-term mean seasonal variations and the expected head values once the aquifer reaches an equilibrium during pumping conditions. This approach is consistent with the goals of this investigation.

	Monitoring Well Average Monthly Hydraulic Head Over 10 Years (m)								
	F7	**F9**	**F11**	**F17**	**F19**	**F20**	**F34**	**F35**	**MF2**
January	31.68	25.71	7.97	13.66	13.24	12.43	11.10	9.47	11.13
February	32.28	26.53	9.14	13.68	14.14	13.29	12.54	10.68	12.51
March	32.38	26.80	9.48	13.61	14.37	13.52	13.06	11.14	13.09
April	32.27	27.04	10.20	13.51	14.82	12.84	12.61	10.58	13.11
May	32.03	26.82	9.68	18.01	14.37	12.54	12.19	10.00	12.94
June	31.68	26.45	8.63	21.57	13.44	12.68	11.12	8.87	12.47
July	31.20	25.85	6.29	20.01	11.73	10.91	9.75	7.46	11.67
August	30.78	25.14	4.62	16.76	10.46	9.70	8.33	6.09	10.77
September	30.36	24.58	5.17	14.13	10.43	9.60	8.26	6.20	10.00
October	30.18	24.23	5.12	13.99	10.43	9.57	8.32	6.50	9.46
November	30.27	24.19	5.45	14.13	10.67	10.01	8.04	6.69	9.37
December	30.72	24.79	6.12	13.90	11.36	10.95	8.86	7.35	9.75

Table 3: *Average monthly hydraulic head values in each monitoring well over 10 years used as observations in the OBS Package in MODFLOW for model calibration. Wells with observations beginning during the model simulation time (1991 to 1997) are used in our numerical model. The 10 year average begins at the first observation and ends after the 10 years. The monitoring wells are in various locations and units surrounding the pumping site. Data from the H+ Hydrogeologic Network.*

The Ploemeur hydrogeological site underwent approximately 20 m of drawdown surrounding the pumping wells in the fault zone and contact zone during the first six years of

consistent groundwater extraction (Le Borgne et al., 2006; Leray et al., 2013; Roques et al., 2018). We compare the drawdown observed in the field to the drawdown simulated in the model when calibrating and analyzing the fit of hydraulic parameters and thicknesses of structures in the model. Previous authors have found that the head values are generally more sensitive to hydraulic and geometric parameters of larger scale geologic features such as the contact zone and fault zone than to the less permeable mica-schist and granite (Le Borgne et al., 2004, 2006; Leray et al., 2012, 2013). The hydraulic parameters we calibrate using PEST with ModelMuse are the horizontal and vertical hydraulic conductivities values for the mica-schist, regolith, fault zone, and contact zone. The hydraulic parameters for the Ploemeur granite were not calibrated because of their low sensitivity to changes in hydraulic head, which is likely due to their extremely low hydraulic conductivity (Leray et al., 2012, 2013). The resulting hydraulic parameters from the model calibration are used when determining the final drawdown estimates and performing the particle tracking simulations.

RESULTS

Model and Model Calibration

Using the PEST calibrated parameters, the model results show a maximum of 20 m of drawdown at the end of the first six years of pumping, with a majority of the drawdown occurring within the first year (Figure 8). Maximum drawdown is observed in the contact zone and fault zone because the wells are open along the intersection of these two units. Drawdown continues to occur throughout the six-year model simulation, though we only observe an additional 3 m of drawdown after the first year. These results are comparable to the 20 m of drawdown during the first six years of groundwater extraction recorded in the literature (Le Borgne et al., 2006; Leray et al., 2013; Roques et al., 2018). The simulated drawdown occurs primarily within the contact zone and fault zone, and shows limited drawdown in the surrounding mica-schist and granite bedrocks. However, we see significantly smaller drawdown in the overlying regolith layer, even in the region over top of the pumping zone. The initial head value in the regolith over the pumping zone is 18 m, after the first year the head is 18 m, and at the end of the model simulation after 6 years the head value is 18 m, thus showing little to no change during our model simulation (Figure 9). Thus, on an annual basis, the simulated regolith outputs the recharge at the same rate as it enters the system. No existing wells are open in the regolith, but previous studies have indicated that the regolith dewaters over time. Our results indicate that the regolith is in a state of equilibrium and does not dewater.

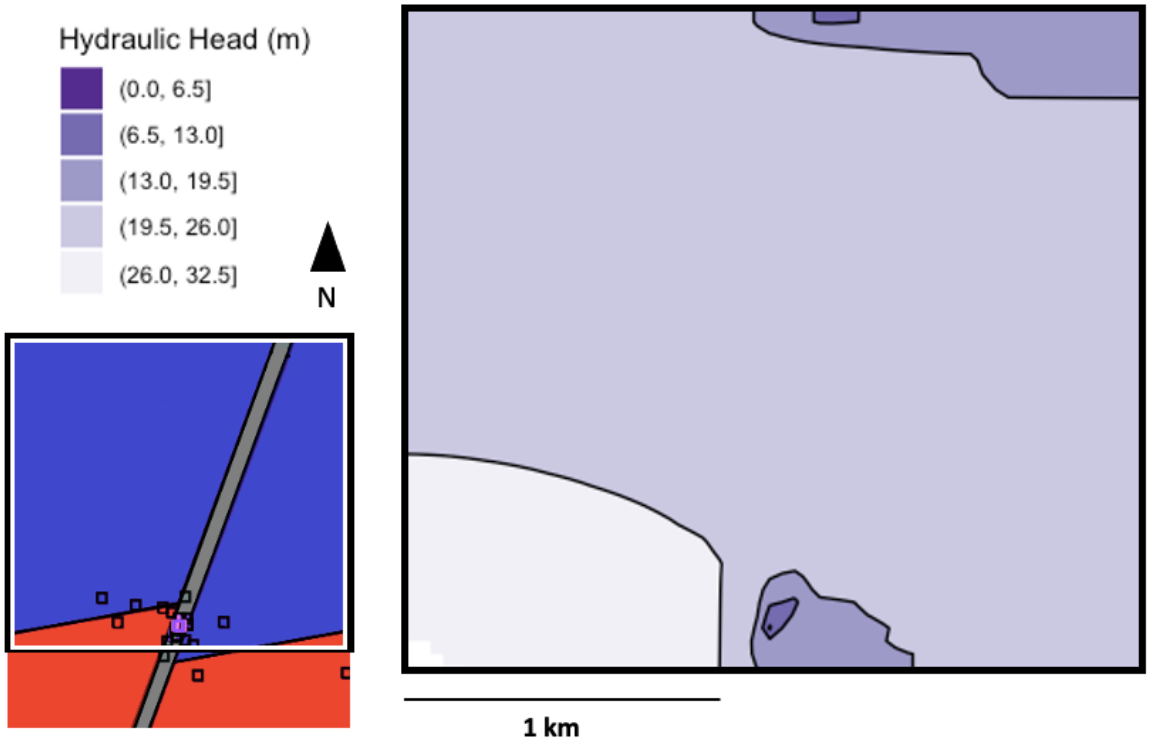

Figure 8: *Hydraulic head values in the contact zone after 6 years of groundwater extraction at the Ploemeur hydrogeologic site. The head in the contact zone varies from -0 m, shown in dark purple surrounding the locations of the pumping wells, to 32.5 m, shown in light purple. The results in the contact zone from the pumping site northward are shown only because the contact zone reaches the surface and pinches out just south of the pumping zone. Figure of hydraulic head contours made in RStudio (RStudio Team, 2020).*

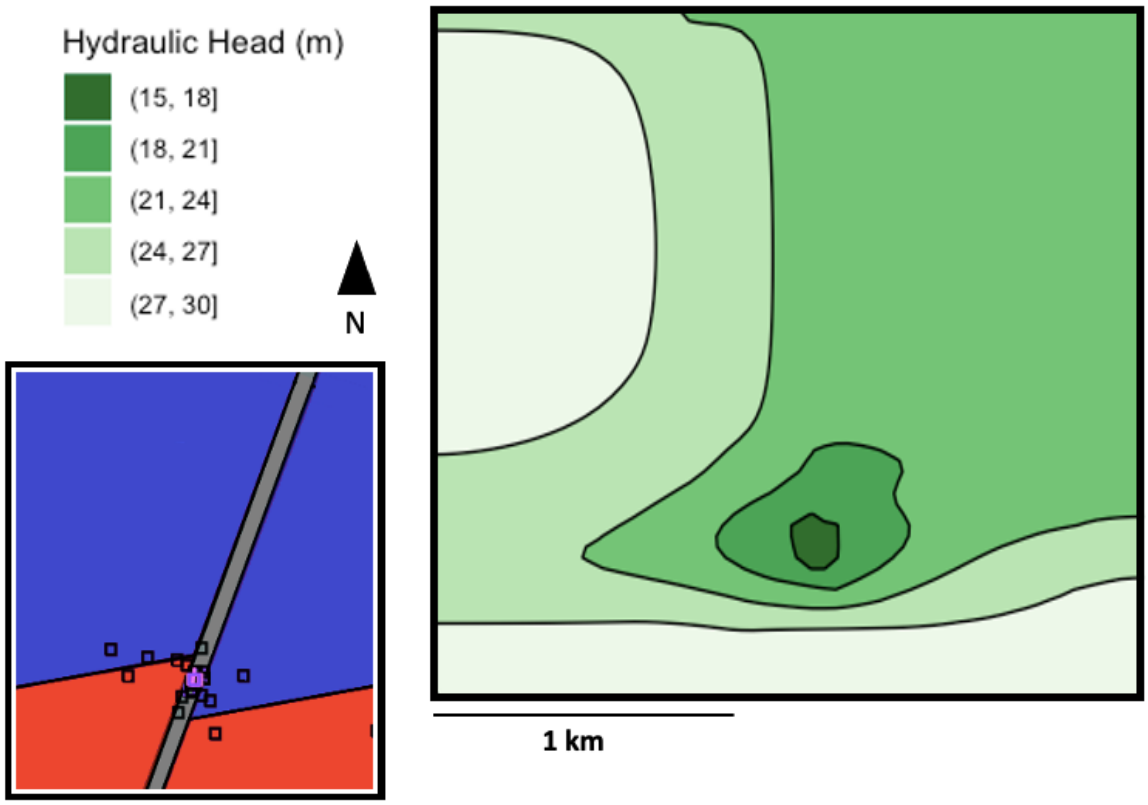

Figure 9: *Hydraulic head values in the regolith after 6 years of groundwater extraction at the Ploemeur hydrogeologic site. The head in the regolith zone varies from 15 m, shown in dark green surrounding the locations of the pumping wells in the region of lowest elevation, to 30 m, shown in light green. Figure of hydraulic head contours made in RStudio (RStudio Team, 2020).*

We also observe consistent inflows and outflows at the northern and southern boundaries to keep the hydraulic head values at the boundaries steady. Throughout the time of the model simulation, the influence of the GHBs increases; the GHBs allow more inflow to the system in the later years of the simulation. The GHB with the strongest influence is located in the contact zone on the northern boundary of the model. We also observe limited inflow through the fault zone, revealing that the GHB at the model margins of the fault zone does not contribute significant quantity of water to the system. There is more outflow than inflow at all of the GHBs. This result

can be attributed to the variations in precipitation and inflow throughout the seasons at the Ploemeur hydrogeologic site. This also shows that pumping from the pumping zone, which is nearly two kilometers away from the northern GHBs and one kilometer away from the southern GHBs, affects the hydraulic head values on the northern and southern borders of the model domain. The inflows from the GHBs, especially those in regions of higher elevation, contribute to the water extracted from the pumping wells and therefore suggests that some pumped water comes through the contact zone from beyond the model boundary.

Model calibration completed with PEST with ModelMuse provides calibrated estimates of hydraulic parameters for the mica-schist, contact zone, fault zone, and regolith (Table 4). The most significant changes in hydraulic parameters from the initial estimates occur with the horizontal hydraulic conductivities of the regolith, mica-schist, and fault zone with all changing by at least one order of magnitude. The vertical hydraulic conductivity in all units and the horizontal hydraulic conductivity of the contact zone were minimally altered, if at all, during calibration, indicating they are either less sensitive in the model or are already well estimated based on previous calibrated models used when conceptualizing this study (Leray et al., 2012). A sensitivity analysis completed with PEST during calibration shows that the horizontal hydraulic conductivity of the fault zone is the most sensitive to the inputted head observations and surrounding geology, while the horizontal hydraulic conductivity of the contact zone and the vertical hydraulic conductivities of all units are the least sensitive. It is important to note that not all simulated head values during calibration were equal to the inputted observations with a variance of up to 13 m.

	Previous Estimates		Calibrated Estimates	
	K_x (m/d)	**K_z (m/d)**	**K_x (m/d)**	**K_z (m/d)**
Regolith	6.57	0.128	16.1	0.128
Mica-schist	1.0×10^{-4}	8.62×10^{-2}	1.0×10^{-6}	8.62×10^{-2}
Contact zone	86.4	8.6	85.45	8.64
Fault zone	1.08	0.108	0.110	0.108

Table 4: *Resulting hydraulic parameters of model calibration with PEST for ModelMuse (Doherty, 2015; Winston, 2020; Under Beta Testing). The horizontal and vertical hydraulic conductivity values were estimated the geologic units and features. The Ploemeur granite is excluded from model calibration due to its significantly lower value and its non-sensitivity to the model results.*

The Zonebudget analysis provides insights on where a majority of flow occurs in the groundwater system; we analyze the sources of inflows and the destinations of outflows for each geologic unit in the Ploemeur hydrogeologic site (Figure 10). Water flows between each of the geologic features and yields and accommodates water from hydrologic processes including recharge, wells, general-head boundaries (GHBs), and storage. The regolith and mica-schist exhibit the most inflow, while the granite exhibits the least amount of flow. Recharge dominates the inflow to the regolith. The outflow from the pumping wells occurs entirely from within the fault zone based on the water budget fully in the fault zone. We observe that storage plays a significant role in groundwater flow in the fault zone, mica-schist, and regolith at the Ploemeur hydrogeologic site.

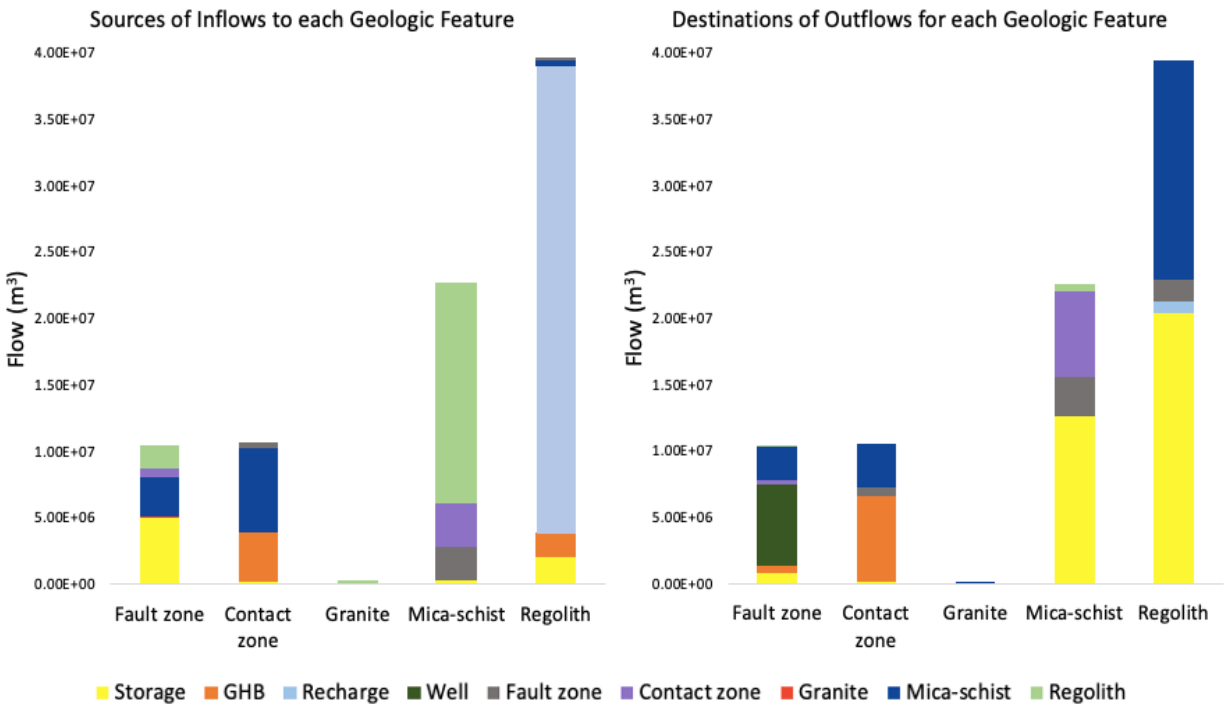

Figure 10: *Total inflows to and outflows from each geologic feature through the six year model simulation calculated with Zonebudget for MODFLOW 6. The sources and destinations include each of the geologic features at the hydrogeologic site, the pumping wells, recharge, the general-head boundaries (GHBs), and storage.*

Further analysis of the storage values estimated in the numerical model with Zonebudget show a decrease in the change in storage in each geologic unit during the six-year simulation period (Figure 11). When the change in storage reaches zero during a transient simulation, that geologic unit has reached equilibrium in the consistent conditions simulated in the model. During the simulated model time of six years, none of the geologic units reach equilibrium. We observe the largest decreases in the change in storage in the mica-schist and contact zone. Based on these trends, the mica-schist will be the first geologic unit to reach equilibrium in an estimated time of 11 years after the commencement of pumping, assuming mean monthly precipitation rates. The fault zone exhibits the smallest change in storage between the beginning and end of the model simulation. The lack of change in the storage in the fault zone is due to the simulated groundwater

extraction occurring in the fault zone, thus preventing it from reaching equilibrium as quickly as the other geologic units. Limited change in storage is also observed in the granite, which is likely due to its low hydraulic conductivity thus reducing its ability to transmit water to other units.

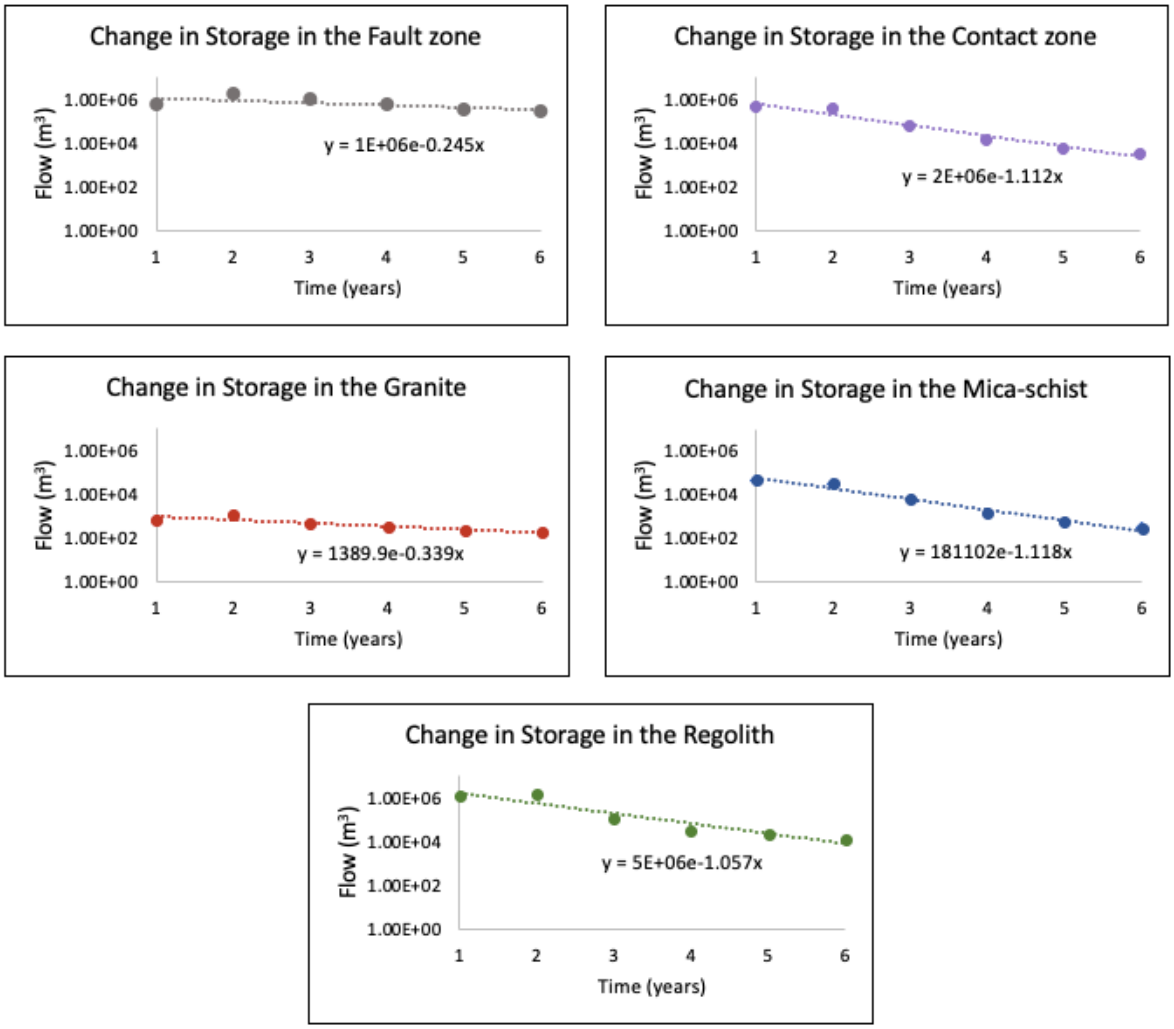

Figure 11: *Change in storage in each of the geologic units during the simulated model time.*

Volumetric flows between each of the five geologic units are also evaluated (Figure 12). Significant flow is simulated to occur between the overlying regolith and the micaschist from recharge infiltration through the regolith and the large shared surface areas between the two units.

The regolith also discharges water to the fault zone as these units are in direct contact, though the quantity is not as great as the contributions between the fault zone and the mica-schist. Both the fault zone and mica-schist are in good communication with the contact zone, and they both lose and receive water from the more permeable contact zone. We observe a high quantity of flow in the contact zone which is due to its comparably large hydraulic conductivity value. The Ploemeur granite does receive water from or lose water to the overlying contact zone and cross-cutting fault zone, and it yields significantly less groundwater flow than the other units due to its extremely low hydraulic conductivity.

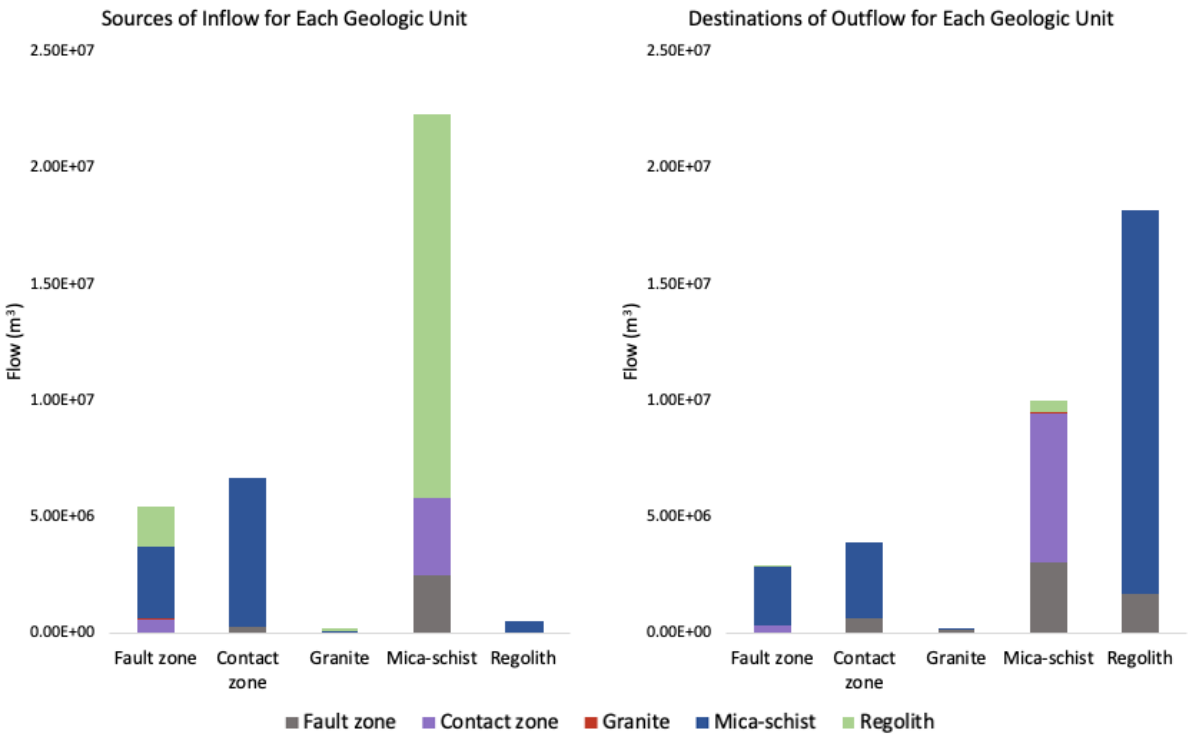

Figure 12: *Total inflows from and outflows to each geologic feature over the six-year simulation period calculated with Zonebudget for MODFLOW 6.*

Particle Tracking Simulations

Backward particle tracking with MODPATH from all three pumping wells shows that the recharge water being extracted from the wells travels from regions of higher land surface elevation, as compared to the elevation at the pumping site, in the northwest and southwest corners through each of the geologic units and features (Figure 13). The simulated water particles appear to preferentially travel through the more permeable geologic units, such as the fault and contact zones. However, significant flow occurs through the mica-schist, and the mica-schist is the preferred pathway compared to the Ploemeur granite. Limited simulated flow is observed to occur through the granite. No particles are simulated to travel to regions east of the pumping wells where lower land surface elevations are widespread. The origins of flow, as indicated by the cross section (Figure 13b.), include the model surface and the GHBs in the contact zone. The backward tracking simulation represents infinite time; thus, it could take decades to centuries for the recharge to reach the pumping wells from the GHBs on the northern model border. The GHBs simulate non-impervious boundaries in the north and south of the model domain, but contribute minimally to water extracted during the pumping wells, particularly during the six-year time span of our model simulation.

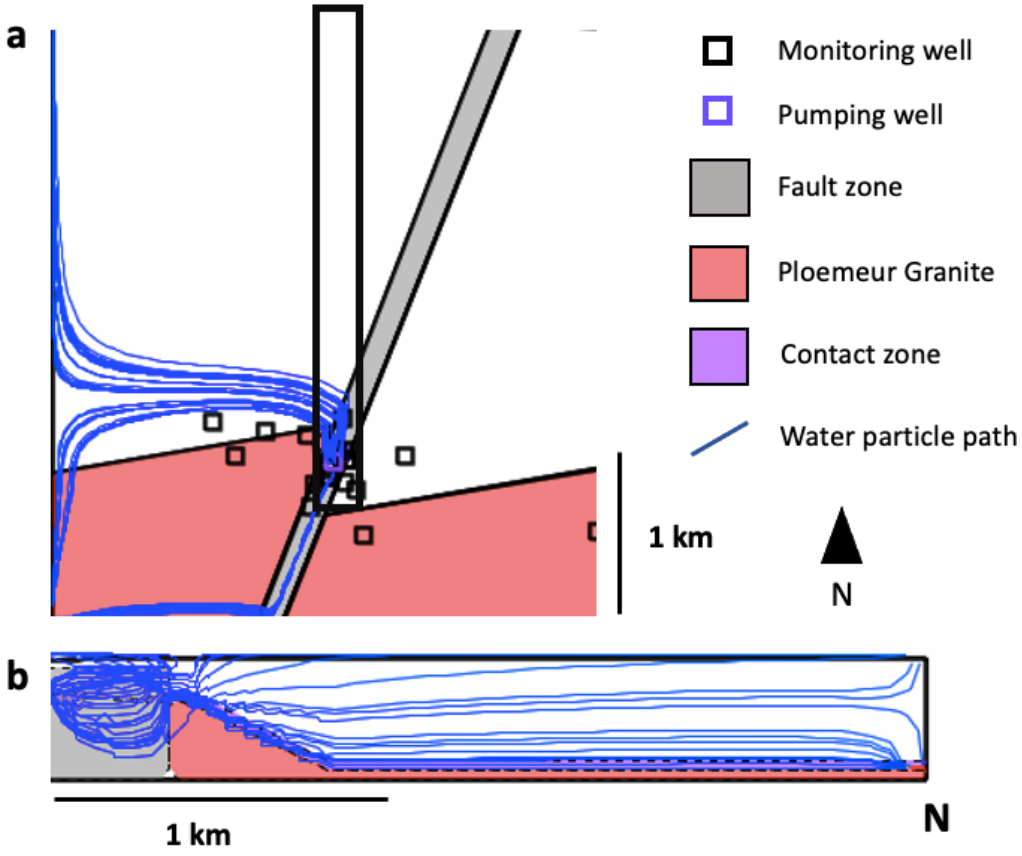

Figure 13: *Backward particle tracking simulation with MODPATH from the pumping wells to their sources of origin.* ***(a.)*** *Map view of the particle tracking simulation. Particles travel from regions of high elevation on the western side of the model area to regions of lower elevation near the pumping well.* ***(b.)*** *Location of the cross section indicated by the box in a. is provided to examine the pathways of subsurface flow for the particle pathways originating in the top northwestern corner.*

A time series analysis was conducted using a backward particle tracking simulation in which the particles originate from the pumping wells (Figure 14). In the six-year simulation period, the water particles are simulated to travel less than 50 m from the pumping well, largely remaining within the fault zone.

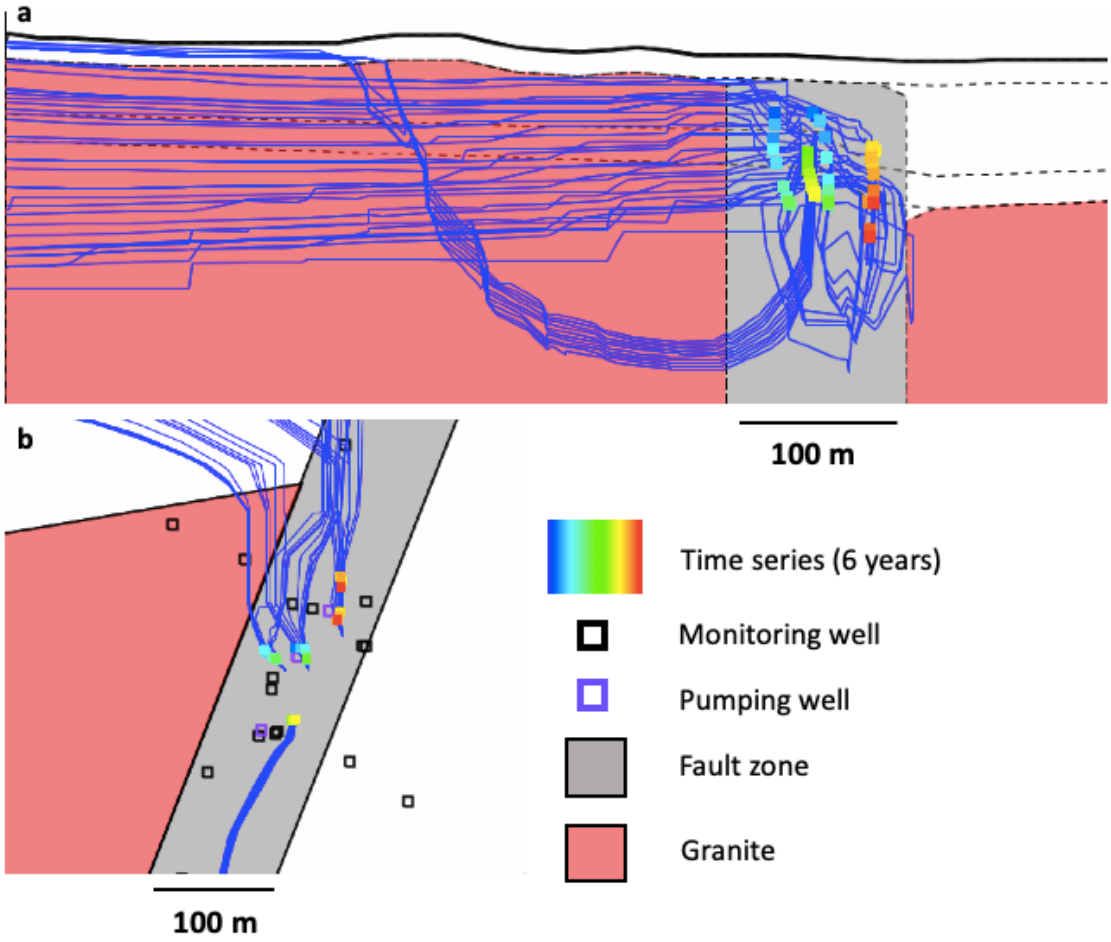

Figure 14: *Time series analysis for the particle path lines simulated during backward tracking from the pumping wells to the source of recharge. The colorful squares represent the location of the simulated water particles after the 6 year model simulation time.* ***(a.)*** *The path lines of particles traveling from the pumping wells to the source of origin from a side view.* ***(b.)*** *The path lines of the particles traveling from the pumping wells to the source of origin from a map view. The simulated water travels between 5 to 40 m during the 6 year model simulation time*

MODPATH particles were implemented at the land surface in the vicinity of the pumping wells to simulate precipitation at the land surface (Figure 15). The particles travelled more quickly (2-4 years) directly above the pumping wells than anywhere else in the simulation due to the steep downward head gradient above the pumping wells and the higher hydraulic conductivity in the fault and contact zones. The particles not simulated on the model surface directly above the

pumping wells travel to the region of lower elevation southeast of the pumping zone. Once the particles reach the region of low elevation, the water percolates through the regolith. The distances the particles travel are functions of the limited simulation time of six years and the hydraulic parameters of the geologic units.

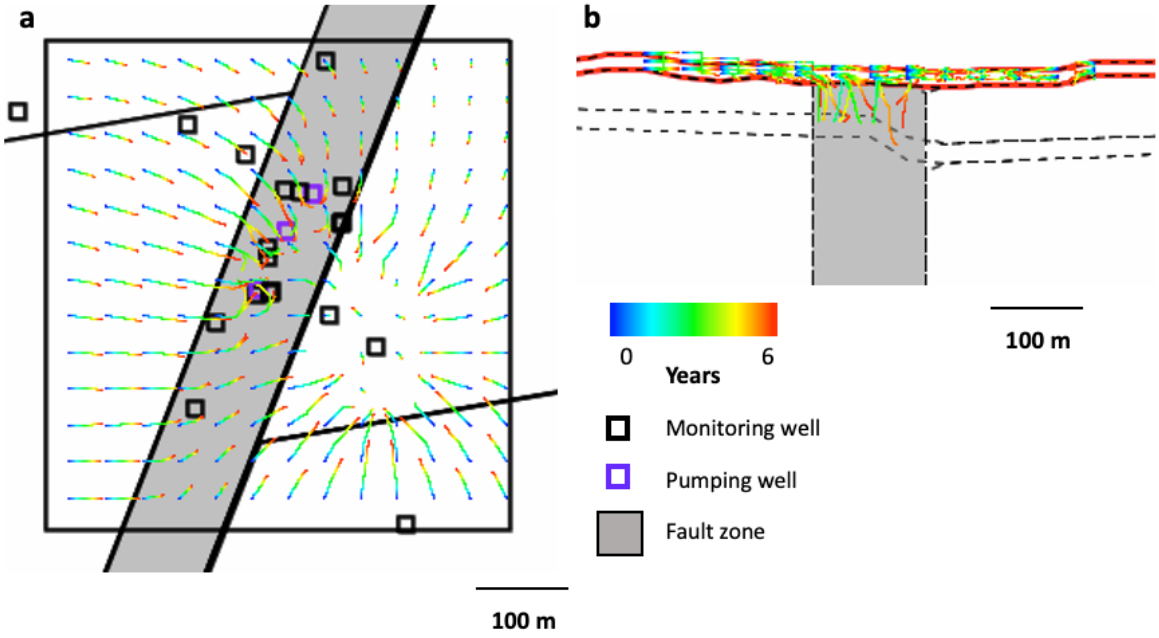

Figure 15: *Forward particle tracking simulation (MODPATH) run above the pumping zone at the Ploemeur hydrogeologic site. Pathways of simulated water particles are shown in a rainbow gradient with blue indicating early time and red indicating late time. The simulation involves using one particle at the surface of each cell and one particle in the middle of each cell.* ***(a.)*** *A map view of the particle tracking forward simulation.* ***(b.)*** *A side view of the particle tracking forward simulation.*

DISCUSSION

A majority of the drawdown is simulated to occur in the more permeable contact and fault zones near the pumping wells. This result is consistent with previous authors who state that wells within the contact zone react more quickly and less intensely to pumping conditions than they do in and around the fault zone (Le Borgne et al., 2004). This is likely due to the hydraulic properties and/or the nature and geometry of the fracturing and heterogeneity in the fault zone (Le Borgne et al., 2004; Leray et al., 2012). Very limited drawdown is simulated to occur within the overlying regolith layer, which is not strongly hydraulically connected to the pumping zone in the intersection of the fault zone and contact zone. The lower hydraulic conductivity in the regolith, due to the presence of mica in the unit, tends to slow horizontal and vertical flow through the unit, which also helps to explain the significant time lag between precipitation and water level response in wells. A majority of the recharge and most of the outflow to other geologic units is simulated to occur in the regolith, which acts as a storage reservoir for the pumping zone through slow gravity drainage to the saturated zone units.

Simulation results from both forward and backward particle tracking reveals that water flow and direction are driven by topographic differences in elevation as it travels laterally from areas of higher elevation to areas of lower elevation as opposed to flowing downward to underlying units. The forward tracking simulation results reveal that water above the pumping wells tends to pool on the surface prior to pumping conditions (Roques et al., 2018). Previous authors also noted that the general flow path in the regolith is from the higher elevations in the northwest part of the study area to the lower elevations of the southeast, which is clearly observed in the simulation of backward tracking particles (Aquilina et al., 2015; Roques et al., 2018). The flow paths show that the simulated particles prefer to move through the more permeable fault and contact zones, but

some water still flows through the less permeable mica-schist and granite. This shows that the crystalline units play a significant role in groundwater flow through the system.

Recharge mechanisms such as piston flow may explain the simulated water pathways observed in the simulations. Piston flow pushes older water out of storage when new water recharges the system, thus storing the new recharge and pushing older water nearer to the pumping wells where it is eventually extracted. Recharge simulated from the model surface above the pumping wells takes between three to six years to penetrate the overlying confining geology and reach the pumping wells. Limited drawdown occurs during the initiation of pumping conditions at the site and in our model. We observe a delayed response in hydraulic head at the Ploemeur site from seasonal changes in precipitation, which is consistent with Jiménez-Martínez et al., (2013) who stated a weak correlation exists between precipitation patterns and hydraulic head response. Therefore, it is evident that the groundwater extracted from the system is not recent precipitation entering the system; instead, the water extracted is likely older water that has been displaced by newer recharge. This result is also consistent with previous authors who found variable residence times throughout the aquifer due to its heterogeneity, with more modern water (<50 years) dominating shallow storage and older water dominating deeper storage and surrounding the contact zone and fault zone (Ayraud et al., 2008; Aquilina et al., 2015; Roques et al., 2018).

Results from all particle tracking simulations reveal it takes a minimum of two years for meteoric water to reach the pumping wells. The simulated particles travel more slowly through the less permeable layers, including the mica schist and granite. Because the simulated recharge can take many years to reach the pumping well, we presume the water extracted from the pumping wells at the beginning of pumping is pulled from the storage of the surrounding geologic units. However, with time, we observe that the change in storage approaches zero in all units, with the

smallest rate of change in the fault zone. Thus, the storage in the fault zone appears to be a primary contributor to the water being extracted through the pumping wells. The storage is then replenished with the recharge water. This result is consistent with the previous observations that much of the extracted water is relatively old water being extracted from the storage deeper in the aquifer system (Ayraud et al., 2008; Aquilina et al., 2015; Roques et al., 2018).

CONCLUSIONS

Though not commonly relied on as prolific water resources, crystalline-rock aquifers can be productive if fractures or other geologic features have hydraulic properties beneficial for holding and transporting water. The Ploemeur hydrogeologic site has unique, intersecting geologic features that allow for limited drawdown during long-term pumping conditions. Because many of the productive features in the Ploemeur aquifer are at depth and contain fractures of unknown aperture and connectivity, a three-dimensional numerical groundwater model of the system is a reliable tool for estimating the hydraulic parameters and flow mechanisms based on field tests and observations.

Modeling results presented in this study reveal the distribution and extent of drawdown, the quantity of patterns and timing of recharge, and the water budget contributions of each geologic feature at the hydrogeologic site. Recharge as meteoric water preferentially travels from regions of high elevation to low elevation through all geologic units, though we observe a preference for groundwater to travel through the more permeable units. Simulated recharge over the pumping site shows that water travels as much as 100 m in two years. Net storage is simulated to steadily decrease over the six-year pumping period in all geologic units, but the smallest change in net storage is observed in the fault zone, where groundwater pumping occurs. Based on water budget calculations from the numerical model, flow to and from storage plays a substantial role in the simulated geologic features. Recharge mechanisms driving flow through the aquifer system consist of both piston flow and preferential flow paths, with piston flow occurring in the crystalline bedrock units and preferential flow dominating in the fractured and permeable contact zone and fault zone. If the annual pumping rate increases or the seasonal precipitation decreases, it is likely that a similar pattern of drawdown and re-equilibration would occur at the site.

Understanding the historical trends and mechanisms of groundwater aquifers, particularly those relied upon by large communities, is an important step toward managing and predicting future groundwater resources. As access to freshwater resources worldwide continue to become more challenging, less relied on groundwater sources, such as crystalline-rock aquifers, will likely become vastly more important. Thus, it is integral understand the recharge mechanisms of crystalline rock aquifers to ensure proper groundwater sustainability and management.

REFERENCES

Abbott, M.B., 1966, An Introduction to the Method of Characteristics. American Elseviers, New York.

Ali, M.H., and Mubarak, S., 2017, Approaches and Methods of Quantifying Natural Groundwater Recharge – A Review, Asian Journal of Environment & Ecology . 5(1): 1-27, 10.9734/AJEE/2017/36987

Alvarado, J. A. C., Leuenberger, M., Kipfer, R., Paces, T. and Purtschert, R., 2011, Reconstruction of past climate conditions over central Europe from groundwater data. Quat. Sci. Rev. **30,** 3423–3429.

Amiotte-Suchet, P., Probst, J.L., and Ludwig, W., 2003, Worldwide distribution of continental rock lithology: implications for the atmospheric/soil CO2 uptake by continental weathering and alkalinity river transport to the oceans. Global Biogeochemical Cycles, v. 17, p. 1038.

Aquilina, L., de Dreuzy, J.-R., Bour, O., Davy, P., 2004. Porosity and fluid velocities in the upper continental crust (2 to 4 km) inferred from injection tests at the Soultz-sous- Forts geothermal site. Geochimica et Cosmochimica Acta 68 (11), 2405–2415 June 1.

Aquilina, L., Vergnaud-Ayraud, V., Labasque, T., Bour, O., Molénat, J., Ruiz, L., de Montety, V., De Ridder, J., Roques, C., Longuevergne, L., 2012. Nitrate dynamics in agricultural catchments deduced from groundwater dating and long-term nitrate monitoring in surface- and groundwaters. Sci. Total Environ. 435–436C:167–178. https://doi.org/ 10.1016/j.scitotenv.2012.06.028.

Aquilina, L., Vergnaud-Ayraud, V., Les Landes, A.A., Pauwels, H., Davy, P., Pételet- Giraud, E., Labasque, T., Roques, C., Chatton, E., Bour, O., BenMaamar, S., Dufresne, A., Khaska, M., La Salle, C.L.G., Barbecot, F., 2015, Impact of climate changes during the last 5 million years on groundwater in basement aquifers: Scientific Reports, v. 5, p. 14132, doi:10.1038/srep14132.

Aquilina, L., Roques, C., Boisson, A., Vergnaud-Ayraud, V., Labasque, T., Pauwels, H., Bour, O., 2018, Autotrophic denitrification supported by biotite dissolution in crystalline aquifers (1): New insights from short-term batch experiments: Science of The Total Environment, v. 619–620, p. 842–853, doi:10.1016/j.scitotenv.2017.11.079.

Ayraud, V., Aquilina, L., Labasque, T., Pauwels, H., Molenat, J., Pierson-Wickmann, A.-C., Durand, V., Bour, O., Tarits, C., Le Corre, P., 2008. Compartmentalization of physical and chemical properties in hard-rock aquifers deduced from chemical and ground- water age analyses. Appl. Geochem. 23:2686–2707. https://doi.org/10.1016/ j.apgeochem.2008.06.001.

Baker, T.J., and Miller, S.N., 2013, Using the soil and water assessment tool (SWAT) to assess land use impact on water resources in an East African watershed, J. of Hydrology, v. 486, p. 100–111.

Bense, V. F., Gleeson, T., Loveless, S. E., Bour, O., and Scibek, J., 2013, Earth-Science Reviews Fault zone hydrogeology, Earth Science Reviews, v. 127, p. 171–192. https://doi.org/10.1016/j.earscirev.2013.09.008

Berkowitz, B., 2002, Characterizing flow and transport in fractured geological media: A review, Advances in Water Resources, v. 25, p. 861-884.

Biessy, G., Moreau, F., Dauteuil, O., and Bour, O., 2011, Surface deformation of an intraplate area from GPS time series: Journal of Geodynamics, v. 52, p. 24–33, doi:10.1016/j.jog.2010.11.005.

Blatt, H. and Jones, R.L., 1975, Proportions of exposed igneous, metamorphic, and sedimentary rocks, Geological Society of America Bulletin, v. 86, p. 1085-1088.

Bour, O., Davy, P., Darcel, C, and Odling, N., 2002, A statistical scaling model for fracture network geometry, with validation on a multiscale mapping of a joint network (Hornelen Basin, Norway), Journal of Geophysical Research: Solid Earth, v. 107, no. B6.

Bouwer, H. 1978. Groundwater Hydrology. McGraw-Hill Book Company, New York

Buckingham E., 1907, Studies on the Movement of Soil Moisture, USDA Bureau of Soils: Washington, v. 38.

Buttle, J.M. and Sami, K., 1990, Recharge Processes During Snowmelt: An Isotopic and Hydrometric Investigation. Hydrological Processes, v. 4, p. 343 - 360.

Caine J.S., Evans, J.P., and Forester, C.B., 1996, Fault zone architecture and permeability structure, Geology, v. 18, p. 1025-1028.

Childs, E.C. and Collis-George, N., 1950, The permeability of porous materials, Proceedings Royal Society London, Series A, v. 201, p. 392 – 405.

Clauser, C., 1992. Permeability of crystalline rocks. Eos, Trans. Am. Geophys. Union 73, no. 21, p. 233–240.

Cook, P.G., 2003. A Guide to Regional Groundwater Flow in Fractured Rock Aquifers.

Courtois, N., Lachassagne, P., Wyns, R., Blanchin, R., Bougaïré, F.D., Somé, S., Tapsoba, A., 2010. Large-scale mapping of hard-rock aquifer properties applied to Burkina Faso. Ground Water, v. 48, no. 2, p. 269–283.

Darcy, H., 1856, Les fontaines publiques de la ville de Dijon. Dalmont. Paris

Day-Lewis, F.D., Hsieh, P.A., and Gorelick, S.M., 2000, Identifying fracture-zone geometry using simulated annealing and hydraulic connection data, Water Resources Research, v. 36 no, 7, p. 1707– 1721.

Day-Lewis, F.D., Lane Jr., J.W., Harris, J.M., and Gorelick, S.M., 2003, Time-lapse imaging of saline-tracer transport in fractured rock using the difference-attenuation radar tomography, Water Resources Research, v. 39, no. 10.

de Dreuzy, J.R., Davy, P., and Bour, O., 2002, Permeability of 2D fracture networks with power-law distributions of length and aperture, Water Resources Research, v. 38, no. 12.

de Dreuzy, J.-R., Davy, P., Erhel, J., and de Bre´mond d'Ars, J., 2004, Anomalous diffusion exponents in continuous 2D multifractal media, Physical Review E, v. 70.

Dewandel, B., Lachassagne, P., Wyns, R., Maréchal, J.C., Krishnamurthy, N.S., 2006, A generalized 3-D geological and hydrogeological conceptual model of granite aquifers controlled by single or multiphase weathering, Journal of Hydrology, v. 330, no. 1–2, p. 260-284

Dewandel, B., Maréchal, J., Bour, O., Ladouche, B., Ahmed, S., Chandra, S., & Pauwels, H., 2012, Upscaling and regionalizing hydraulic conductivity and effective porosity at watershed scale in deeply weathered crystalline aquifers, Journal of Hydrology, v. 416, p. 83-97.

Doherty, J., 2015, PEST - The Book: Calibration and Uncertainty Analysis for Complex Environmental Models. Watermark Numerical Computing, Brisbane, Australia, ISBN: 978-0-9943786-0-6, 227 p.

Evans, J.P., Forster, C.B., Goddard, J.V., 1997. Permeability of fault-related rocks, and implications for hydraulic structure of fault zones. J. Struct. Geol. 19, 1393–1404.

Farkas-Karay, G. and Hajnal, G., 2015, Modelling of Groundwater Flow in Fractured Rocks: Procedia Environmental Sciences, v. 25, p. 142-149, doi: 10.1016/j.proenv.2015.04.020.

Freeze, R., and Cherry, J., 1979, Groundwater, Old Tappan, New Jersey: Prentice-Hall.

Gee, G.W. and Hillel, D., 1988, Groundwater Recharge in Arid Regions: Review and Critique of Estimation Methods. Hydrological Processes, v. 2, p. 255-266.

Gleeson, T., Novakowski, K., & Kurt Kyser, T., 2009, Extremely rapid and localized recharge to a fractured rock aquifer, Journal of Hydrology, v. 376, no. 3–4, p. 496–509.

Gleeson, T., Smith, L., Moosdorf, N., Hartmann, J., Duerr, H.H., Manning, A.H., van Beek, L.P.H., and Jellinek, A.M., 2011, Mapping permeability over the surface of the Earth., Geophysical Research Letters, v. 38, no. L02401.

Gleeson, T.R., Wada, Y., Bierkens, M.F.P, van Beek, L.P.H., 2012, Water balance of global aquifers revealed by groundwater footprint, Nature, v. 488, p. 197–200. doi:10.1038/nature11295

Green, T. R., Taniguchi, M., Kooi, H., Gurdak, J.J., Allen, D.M., Hiscock, K.M., Treidel, H., and Aureli, Al., 2011,. Beneath the surface of global change: Impacts of climate change on groundwater. Journal of Hydrology, v. 405, p. 532–560, doi:https://doi.org/10.1016/j.jhydrol.2011.05.002

Guymon, G.L., 1994. Unsaturated zone hydrology, Prentice Hall, Englewood Cliffs, New Jersey, 210 pp.

Harbaugh, A.W., 1990, A computer program for calculating subregional water budgets using results from the U.S. Geological Survey modular three-dimensional ground-water flow model: U.S. Geological Survey Open-File Report 90-392, 46 p.

Haverkamp, R., Bouraoui, F., Zammit, C., and Angulo-Jaramillo, R., 1999, Soil Properties and Movement in the Unsaturated Zone, in J.W. Delleur (ed.), The handbook of Ground-water Engineering. CRC: Boca Raton, ch. 5.

Healy, R.W., 2010, Estimating groundwater recharge, Cambridge University Press, Cambridge .

Hewlett, J.D. and Hibbert, A.R., 1967, Factors affecting the response of small watersheds to precipitation in humid areas, In Sopper, W.E. and Lull, H.W., editors, Forest hydrology, New York: Pergamon Press, p. 275—90.

Hornberger, G. M., Raffensperger, J. P., Wilberg, P. L., and Eshleman, K. N., 1998: Elements of Physical Hydrology. The Johns Hopkins University Press, 302 pp.

Hughes, J.D., Langevin, C.D., and Banta, E.R., 2017, Documentation for the MODFLOW 6 framework: U.S. Geological Survey Techniques and Methods, book 6, chap. A57, 42 p., https://doi.org/10.3133/tm6A57.

Jiménez-Martínez, J., Longuevergne, L., Le Borgne, T., Davy, P., Russian, A., and Bour, O., 2013, Temporal and spatial scaling of hydraulic response to recharge in fractured aquifers: Insights from a frequency domain analysis: Temporal and Spatial Scaling in Fractured Aquifers: Water Resources Research, v. 49, p. 3007–3023, doi:10.1002/wrcr.20260.

Kiraly, L., 1975. Rapport sur l'e´tat actuel des connaissances dans le domaine des caractéres physiques des roches karstiques, In: Burger, A., Dubertret, L. (Eds.), Hydrogeology of Karstic Terrains, International association of hydrogeologists, Paris.

Klump, S., Grundl, T., Purtschert, R. and Kipfer, R., 2008, Groundwater and climate dynamics derived from noble gas, C-14, and stable isotope data, Geology, v. 36, p. 395–398.

Lamur, A., Kendrick, J., Eggertsson, G., Wall, J.R., Ashworth, D.J., and Lavallée, Y., 2017, The permeability of fractured rocks in pressurized volcanic and geothermal systems, Scientific Reports, v. 7.

Langevin, C.D., Hughes, J.D., Banta, E.R., Niswonger, R.G., Panday, Sorab, and Provost, A.M., 2017, Documentation for the MODFLOW 6 Groundwater Flow Model: U.S. Geological Survey Techniques and Methods, book 6, chap. A55, 197 p., https://doi.org/10.3133/tm6A55.

Langevin, C.D., Hughes, J.D., Banta, E.R., Provost, A.M., Niswonger, R.G., and Panday, Sorab, 2021, MODFLOW 6 Modular Hydrologic Model version 6.2.1: U.S. Geological Survey Software Release, 18 February 2021 https://doi.org/10.5066/F76Q1VQV

Law, S., 2019, A Numerical and Statistical Analysis of the Fractured Rock Aquifer System in Ploemeur, France to Quantify Local and Regional Recharge: Virginia Tech, 60 p.

Le Borgne, T., Bour, O., de Dreuzy, J.R., Davy, P., and Touchard, F., 2004, Equivalent mean flow models for fractured aquifers: Insights from a pumping tests scaling interpretation: EQUIVALENT MEAN FLOW MODELS: Water Resources Research, v. 40, doi:10.1029/2003WR002436.

Le Borgne, T., Bour, O., Paillet, F.L., and Caudal, J.P., 2006, Assessment of preferential flow path connectivity and hydraulic properties at single-borehole and cross-borehole scales in a fractured aquifer: Journal of Hydrology, v. 328, p. 347–359, doi:10.1016/j.jhydrol.2005.12.029.

Lee, L.J.E., Lawrence, D.S.L., and Price, M., 2006, Analysis of water-level response to rainfall and implications for recharge pathways in the Chalk aquifer, SE England, J. Hydrol., v. 330, p. 604–20

Leray, S., de Dreuzy, J.-R., Bour, O., and Bresciani, E., 2013, Numerical modeling of the productivity of vertical to shallowly dipping fractured zones in crystalline rocks: Journal of Hydrology, v. 481, p. 64–75, doi:10.1016/j.jhydrol.2012.12.014.

Leray, S., de Dreuzy, J.-R., Bour, O., Labasque, T., and Aquilina, L., 2012, Contribution of age data to the characterization of complex aquifers: Journal of Hydrology, v. 464–465, p. 54–68, doi:10.1016/j.jhydrol.2012.06.052.

Lerner, D.N., Issar, S.A., and Simmers, I., 1990, Groundwater recharge – a guide to understanding and estimating natural recharge, Heise, Hannover, 345 pp.

Lerner, D.N., 2002, Identifying and quantifying urban recharge: A review, Hydrogeology Journal, v. 10, p. 143-152.

Lloyd, J.W., 1986, A review of aridity and groundwater, Hydrol. Process., v. 1, p. 63-78.

Maréchal, J.C., Dewandel, B., Subrahmanyam, K., 2004. Contribution of hydraulic tests at different scales to characterize fracture network properties in the weathered-fissured layer of a hard rock aquifers. Water Resour. Res. 40, W11508.

Maréchal, J.C., Selles, A., Dewandel, B., Boisson, A., Perrin, J., and Ahmed, S., 2018, An Observatory of Groundwater in Crystalline Rock Aquifers Exposed to a Changing Environment: Hyperabad, India, Vadose Zone Journal, v. 17, no. 1, p. 1-14.

Mougin, B., Allier, D., Blanchin,. R., Carn, A., Courtois, N., Gateau, C., and Putot, E., 2008, SILURES Bretagne (Système d'Information pour la Localisation et l'Utilisation des Ressources en Eaux Souterraines) [SILURES Bretagne (Information system for the location and use of groundwater resources in the Armorican Massif)]. Final report, BRGM/RP-56457.

Mustafa, S.M.T., Abdollahi, K., Verbeiren, B., Huysmans, M., 2017, Identification of the influencing factors on groundwater drought and depletion in northwestern Bangladesh. Hydrogeol. J., p. 1–19.

Nimmo, J.R., 2005, Unsaturated Zone Flow Processes, in Anderson, M.G., and Bear, J., eds., Encyclopedia of Hydrological Sciences: Part 13--Groundwater: Chichester, UK, Wiley, v. 4, p. 2299-2322.

Niswonger, R.G., Prudic, D.E., and Regan, R.S., 2006, Documentation of the Unsaturated-Zone Flow (UZF1) Package for modeling unsaturated flow between the land surface and the water table with MODFLOW-2005, USGS Techniques and Methods 6-A19, Reston, Virginia: USGS.

Pedretti, D., Russian, A., Sanchez-Vila, X., and Dentz, M., 2016, Scale dependence of the hydraulic properties of a fractured aquifer estimated using transfer functions, Water Resour. Res., v. 52, p. 5008– 5024.

Pollock, D.W., 2017, MODPATH v7.2.01: A particle-tracking model for MODFLOW: U.S. Geological Survey Software Release, 15 December 2017, http://dx.doi.org/10.5066/F70P0X5X.

Richards, L.A., 1931, "Capillary conduction of liquids through porous mediums," Physics, v. 1, no. 5, p. 318–333.

Roques, C. Aquilina, L., Boisson , A., Vergnaud-Ayraud, V., Labasque, T., Longuevergne, L., Laurencelle, M., Dufresne, A., de Dreuzy, J., Pauwels, H., and Olivier, B., 2018, Autotrophic denitrification supported by biotite dissolution in crystalline aquifers: (2) transient mixing and denitrification dynamic during long-term pumping: Science of The Total Environment, v. 619–620, p. 491–503, doi:10.1016/j.scitotenv.2017.11.104.

Roques, C., Aquilina, L., Bour, O., Maréchal, J., Dewandel, B., Pauwels, H., Labasque, T., Vergnaud-Ayraud, V., Hochreutener, R., 2014. Groundwater sources and geochemical processes in a crystalline fault aquifer. J. Hydrol. 519:3110–3128. https://doi.org/10.1016/j.jhydrol.2014.10.052.

Roques, C., Bour, O., Aquilina, L., and Dewandel, B., 2016, High-yielding aquifers in crystalline basement: insights about the role of fault zones, exemplified by Armorican Massif, France: Hydrogeology Journal, v. 24, p. 2157–2170, doi:10.1007/s10040-016-1451-6.

RStudio Team, 2020, RStudio: Integrated Development for R, RStudio, PBC, Boston, MA, URL http://www.rstudio.com/.

Ruelleu, S., Moreau, F., Bour, O., Gapais, D., and Martelet, G., 2010, Impact of gently dipping discontinuities on basement aquifer recharge: An example from Ploemeur (Brittany, France): Journal of Applied Geophysics, v. 70, p. 161–168, doi:10.1016/j.jappgeo.2009.12.007.

Rugh, D.F., Burbey, T.J. Using saline tracers to evaluate preferential recharge in fractured rocks, Floyd County, Virginia, USA. Hydrogeol J **16,** 251–262 (2008). https://doi.org/10.1007/s10040-007-0236-3

Scanlon, B., Healy, R., and Cook, P.G., 2002, Choosing Appropriate Techniques for Quantifying Groundwater Recharge, Hydrogeology Journal, v. 10, p. 18- 39.

Scibek, J., Allen, D. M., Cannon, A. J. and Whitfield, P. H., 2007, Groundwater-surface water interaction under scenarios of climate change using a high-resolution transient groundwater model. Journal of Hydrology, v. 333, p. 165–181.

Schuite, J., Longuevergne, L., Bour, O., Boudin, F., Durand, S., and Lavenant, N., 2015, Inferring field-scale properties of a fractured aquifer from ground surface deformation during a well test: AQUIFER PROPERTIES FROM DEFORMATION: Geophysical Research Letters, v. 42, p. 10,696-10,703, doi:10.1002/2015GL066387.

Schuite, J., Longuevergne, L., Bour, O., Burbey, T.J., Boudin, F., Lavenant, N., and Davy, P., 2017, Understanding the Hydromechanical Behavior of a Fault Zone From Transient Surface Tilt and Fluid Pressure Observations at Hourly Time Scales: HYDROMECHANICAL BEHAVIOR OF A FAULT: Water Resources Research, v. 53, p. 10558–10582, doi:10.1002/2017WR020588.

Seaton, W.J., and Burbey, T.J., 2005, Influence of ancient thrust faults on the hydrogeology of the Blue Ridge Province, Groundwater, v. 43, no. 3, p. 301-313.

Smith, M., 1993, Neural networks for statistical modeling: New York, Van Nostrand Reinhold, 235 p.

Stober, I. and Bucher, K., 2006, Hydraulic properties of the crystalline basement, Hydrogeology Journal, v. 15, p. 213–24.

Sukhija, B.S., Reddy, D.V., Nagabhushanam, P., and Hussain, S., 2003, Recharge processes: piston flow vs. preferential flow in semi-arid aquifers of India, Hydrogeol J, v. 11, no. 3, p. 387–395

Taylor, R. and Howard, K., 2000, A tectono-geomorphic model of the hydrogeology of deeply weathered crystalline rock: evidence from Uganda, Hydrogeol. J., v. 8, no. 3, p. 279–294.

Tolman, C.F., 1975, Ground Water, McGraw-Hill, New York, 1937, 593 pp.

Touchard, F., 1999, Caractérisation hydrogéologique d'un aquifère de socle fracturé: site de Ploemeur (Morbihan), Ph.D. Thesis, University of Rennes 1, France.

Vigneresse, J.L., 1983, Enracinement des granites armoricains estimés d'après la gravimétrie, Bulletin de la Societé Géologique et Minéralogique de Bretagne, v. 15, p. 1–15.

Wakode, H.B., Baier, K., Jha, R., and Azzam, R., 2018, Impact of urbanization on groundwater recharge and urban water balance for the city of Hyderabad, India, International Soil and Water Conservation Research, v. 6, no. 1.

White, J.T., Hunt, R.J., Fienen, M.N., and Doherty, J.E., 2020, Approaches to Higher Parameterized Inversion: PEST++ Version 5, a Software Suite for Parameter Estimation, Uncertainty Analysis, Management Optimization and Sensitivity Analysis: U.S. Geological Survey Techniques and Methods 7C26, 52 p., https://doi.org/10.3133/tm7C26.

Winston, R.B., 2019, ModelMuse version 4—A graphical user interface for MODFLOW 6: U.S. Geological Survey Scientific Investigations Report 2019–5036, 10 p., https://doi.org/10.3133/sir20195036.

Winston, R.B., 2020, ModelMuse version 4.3: U.S. Geological Survey Software Release, 16 August 2020, https://doi.org/10.5066/P9XMX92F.

Winter, T.C. & Harvey, J.W. & Lehn Franke, O & Alley, William. (1998). Ground water and surface water a single resource: U. U.S. Geol. Surv. Circ.. 1139

Wright, E.P., 1992, The hydrogeology of crystalline basement aquifers in Africa, Geol. Soc. Lond. Spec. Publ., v. 66, p. 1–27. doi:10.1144/GSL.SP.1992.066.01.01

Zimmermann, U., Ehhalt, D., and Muennich, K.O., 1967, Soil-water movement and evapotranspiration: changes in the isotopic composition of the water, Isotopes in Hydrology, pp 567-85. Vienna, International Atomic Energy Agency, 14–18.